Supplementary Materials for "Discovery of High-Performance Thermoelectric Chalcogenides Through First-Principles High-Throughput Screening"

Tao Fan*[a], Artem R. Oganov[a]

[a]Skolkovo Institute of Science and technology, Bolshoy Boulevard 30, bld. 1, Moscow, Russia 121205.

1. $X_4Y_4Z_4$ (X=VIII B, Y=IV A, V A, Z=VI A)

CoAsS

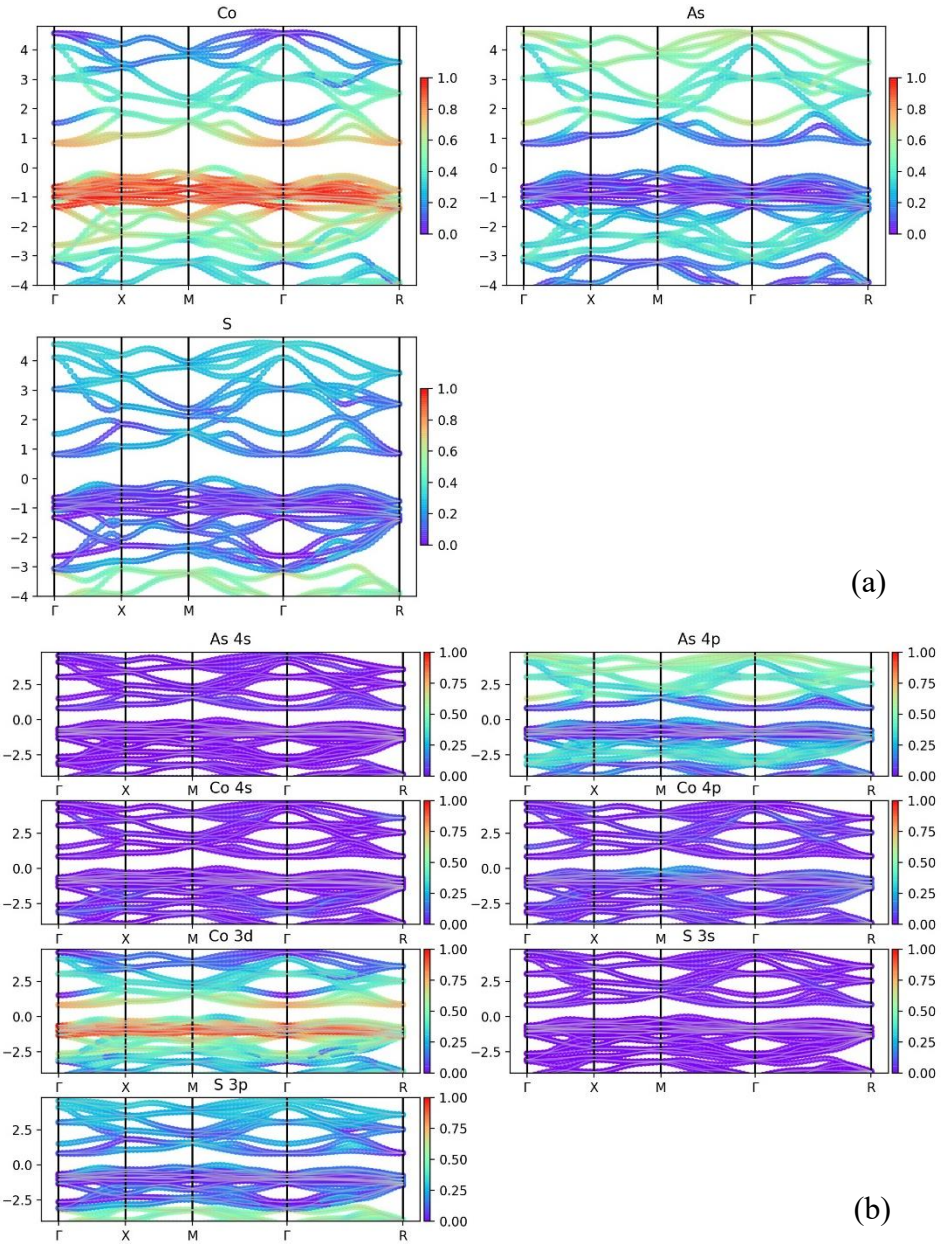

Figure S1: (a) atomic-projected and (b) orbital-projected band structure of CoAsS.

CoAsSe

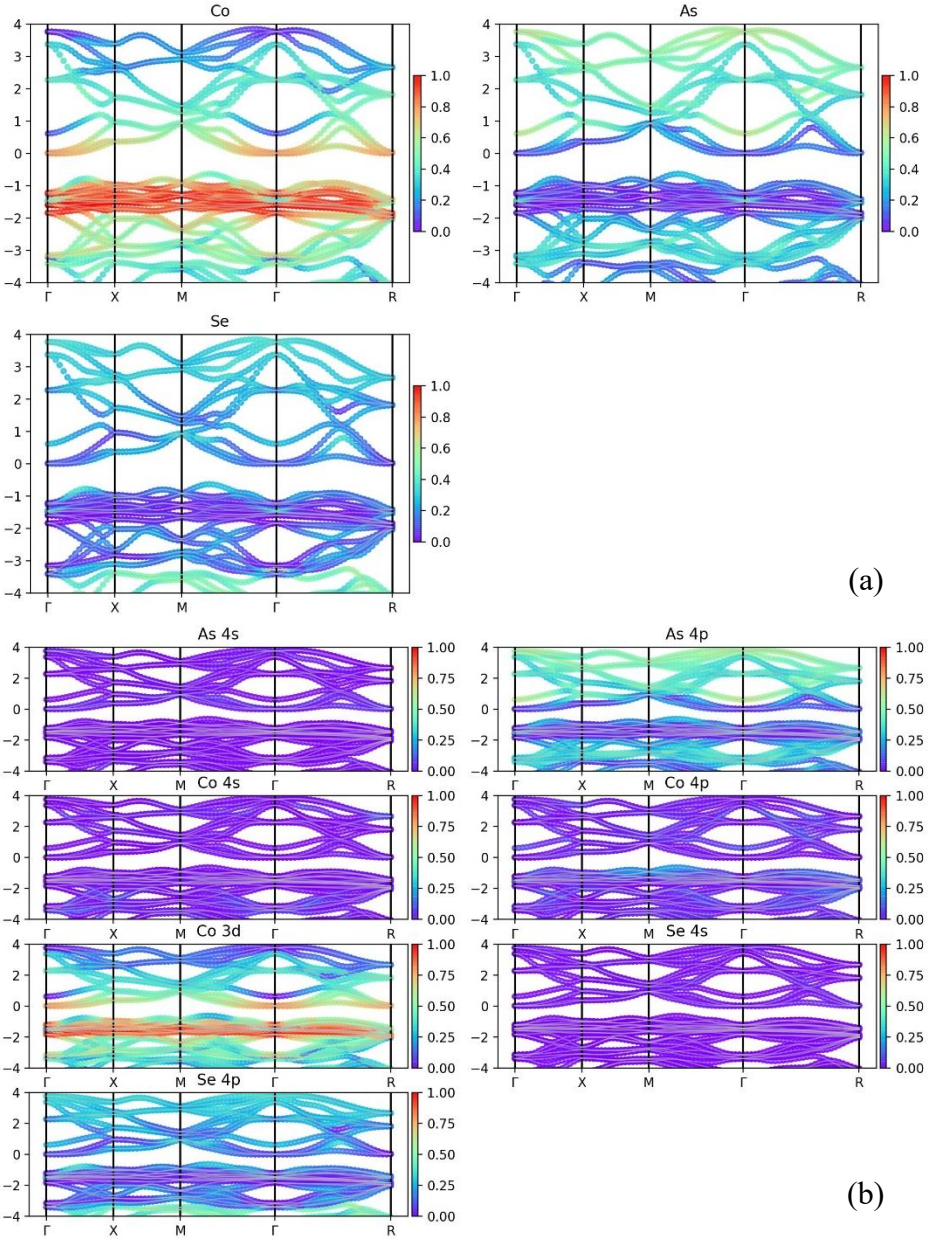

Figure S2: (a) atomic-projected and (b) orbital-projected band structure of CoAsSe.

CoPS

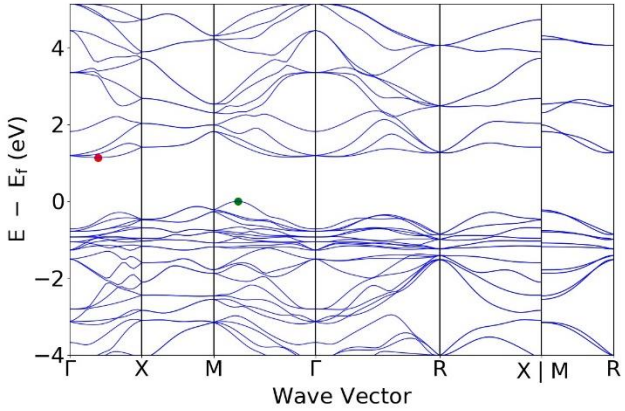

Figure S3: Band structure of CoPS.

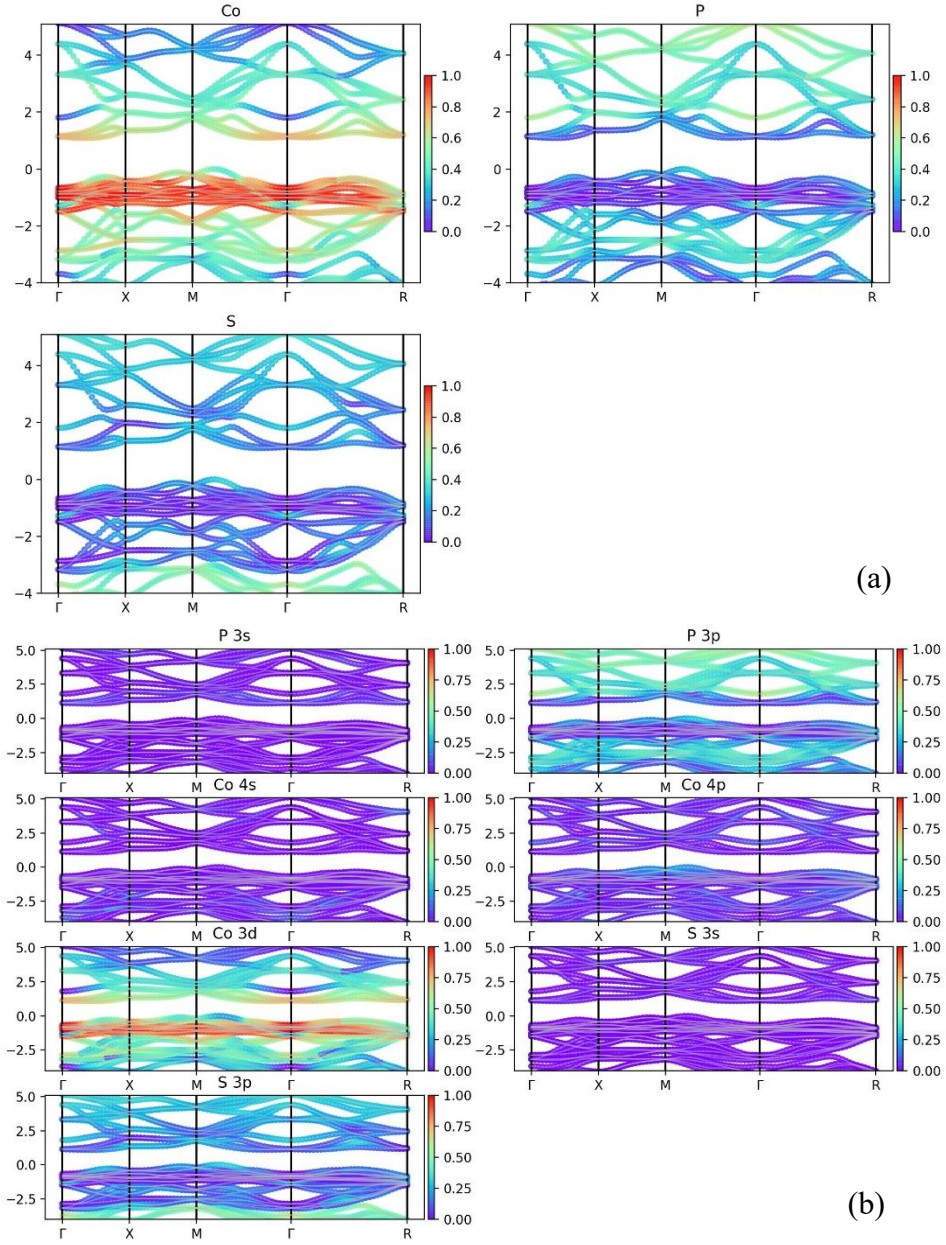

Figure S4: (a) atomic-projected and (b) orbital-projected band structure of CoPS.

CoPSe

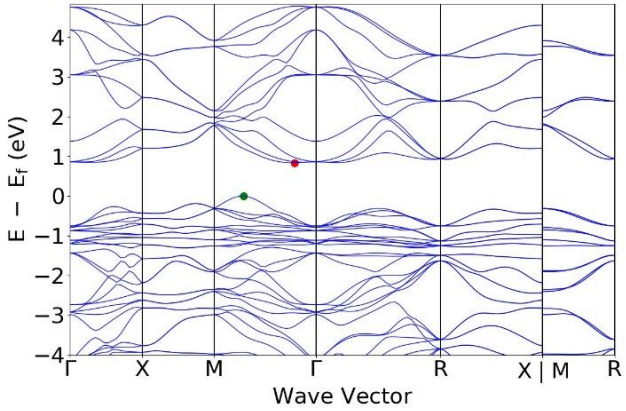

Figure S5: Band structure of CoPSe.

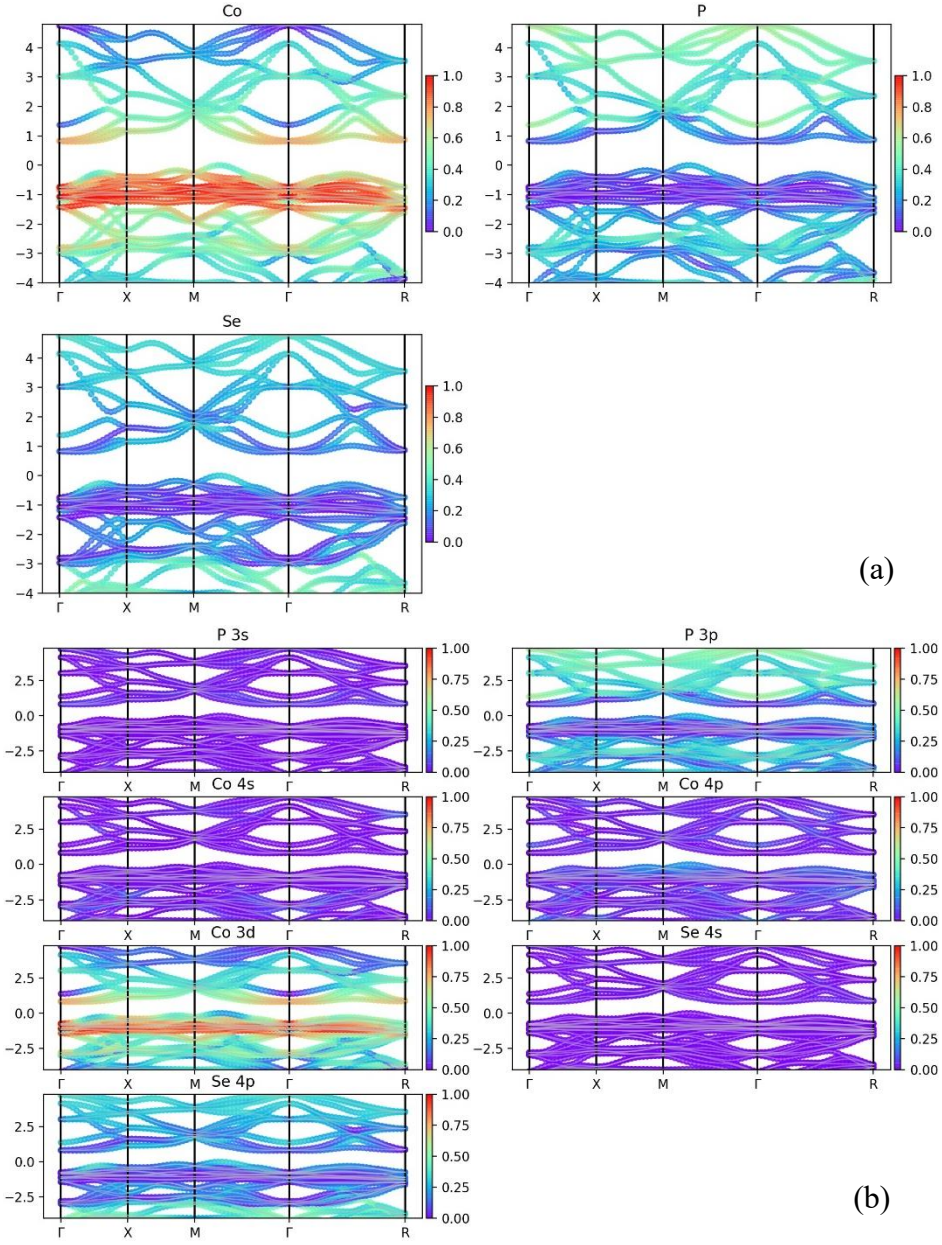

Figure S6: (a) atomic-projected and (b) orbital-projected band structure of CoPSe.

CoSbS

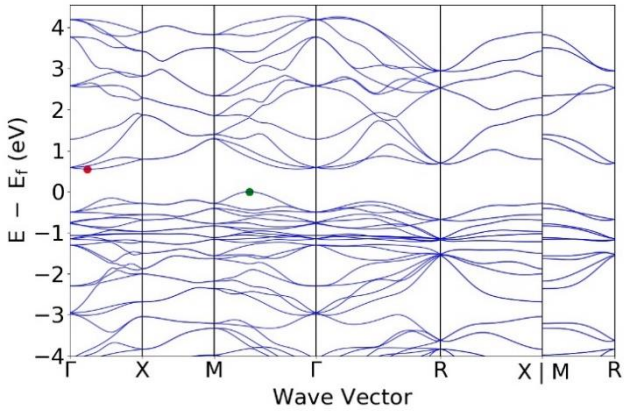

Figure S7: Band structure of CoSbS.

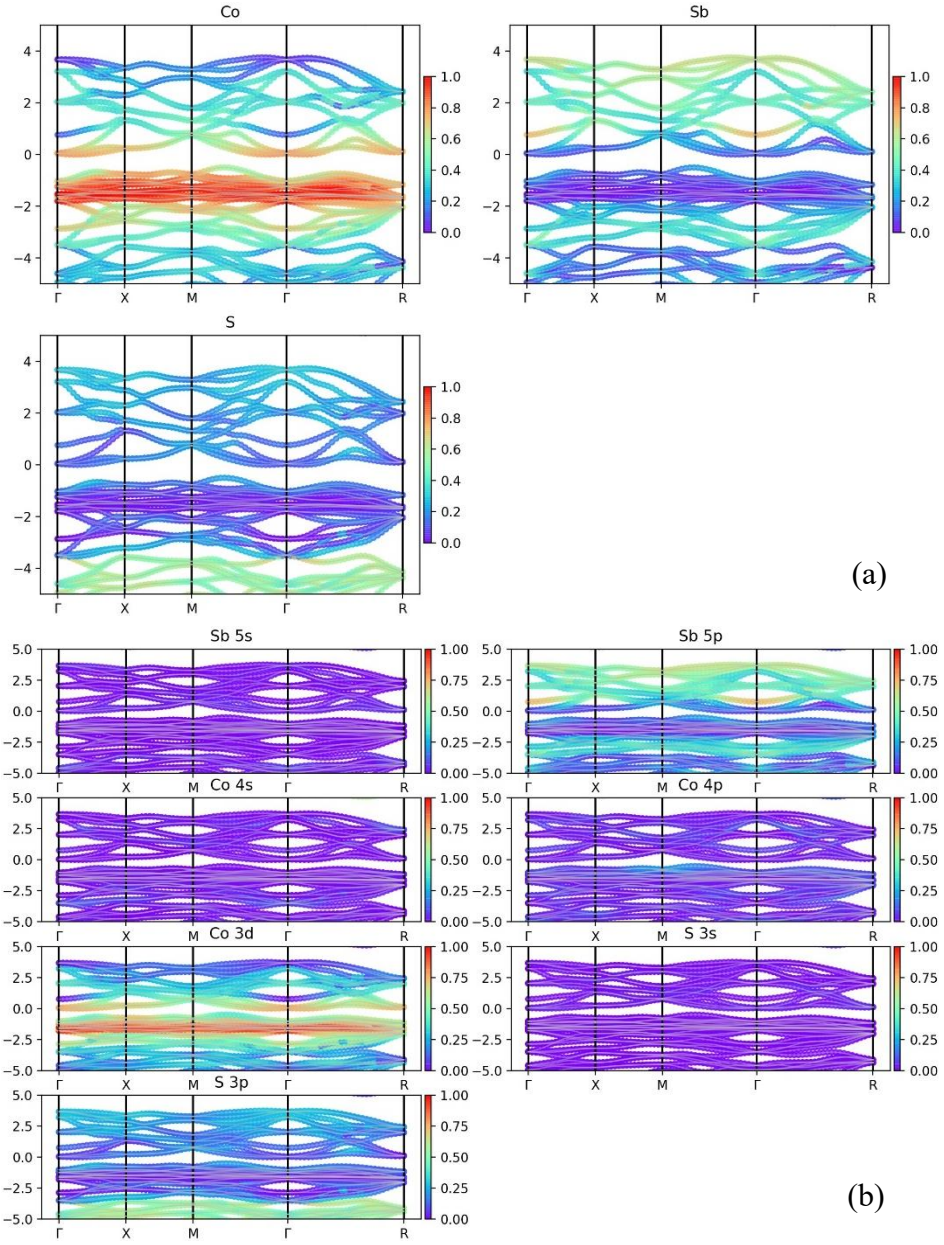

Figure S8: (a) atomic-projected and (b) orbital-projected band structure of CoSbS.

RhAsSe

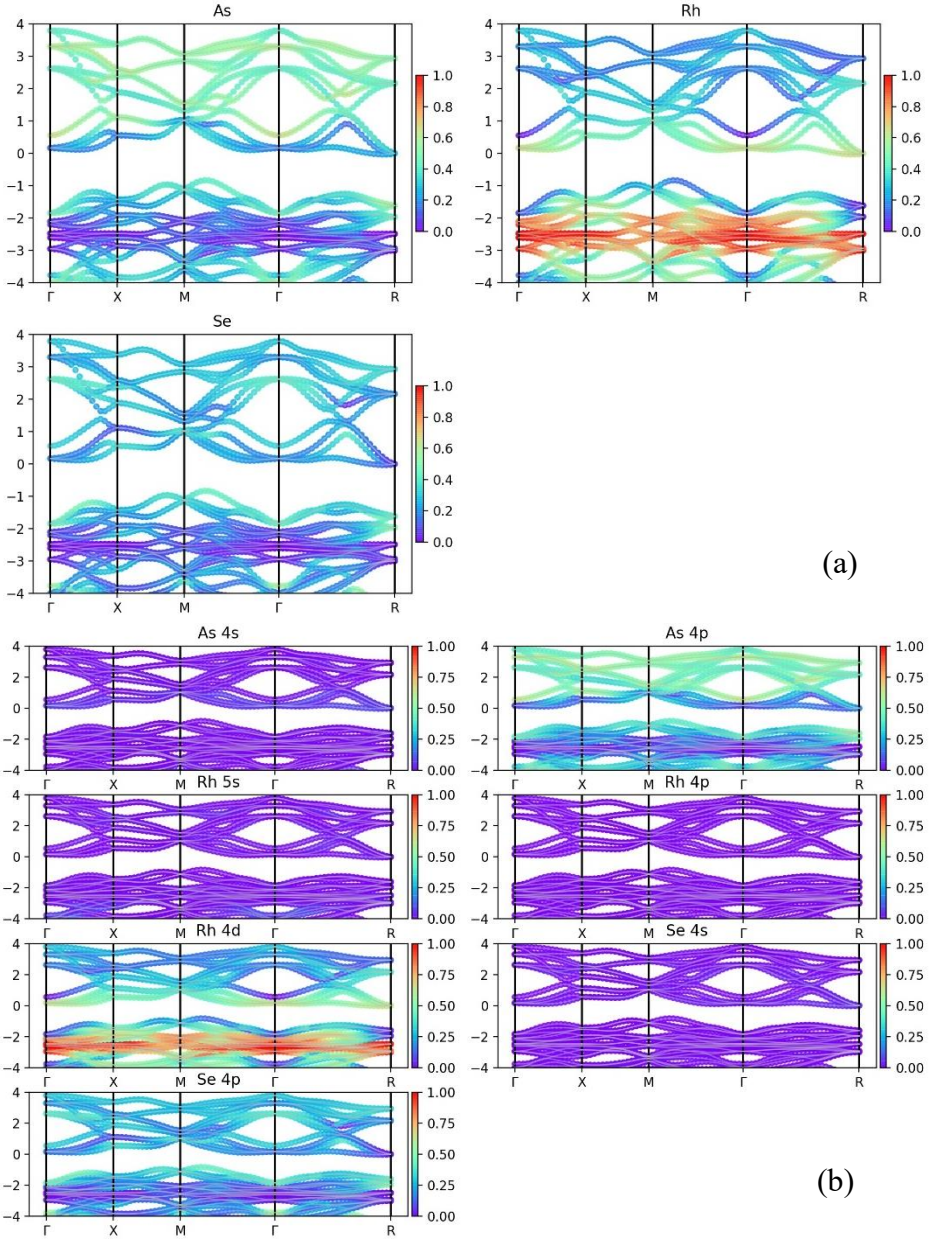

Figure S9: (a) atomic-projected and (b) orbital-projected band structure of RhAsSe.

RhSbTe

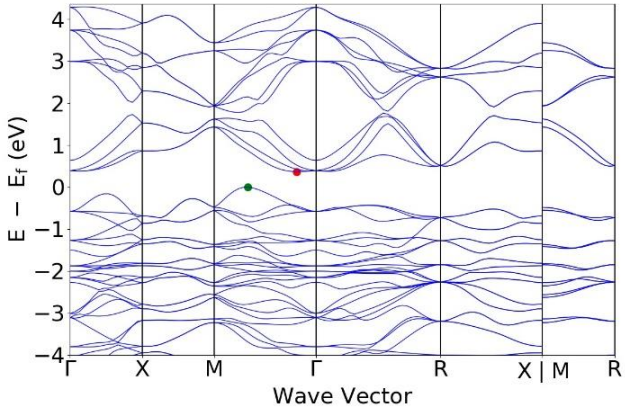

Figure S10: Band structure of RhSbTe.

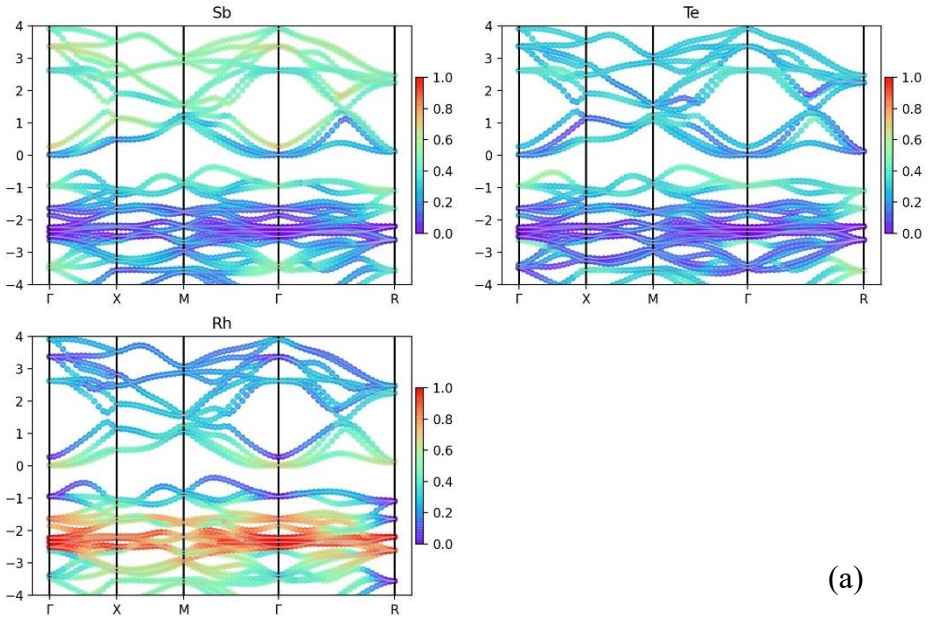

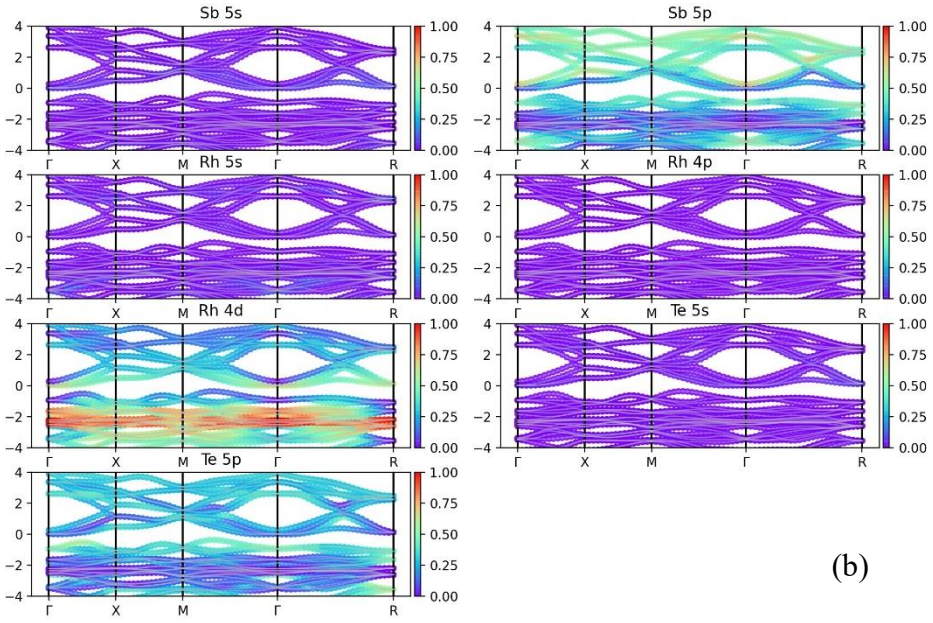

Figure S11: (a) atomic-projected and (b) orbital-projected band structure of RhSbTe.

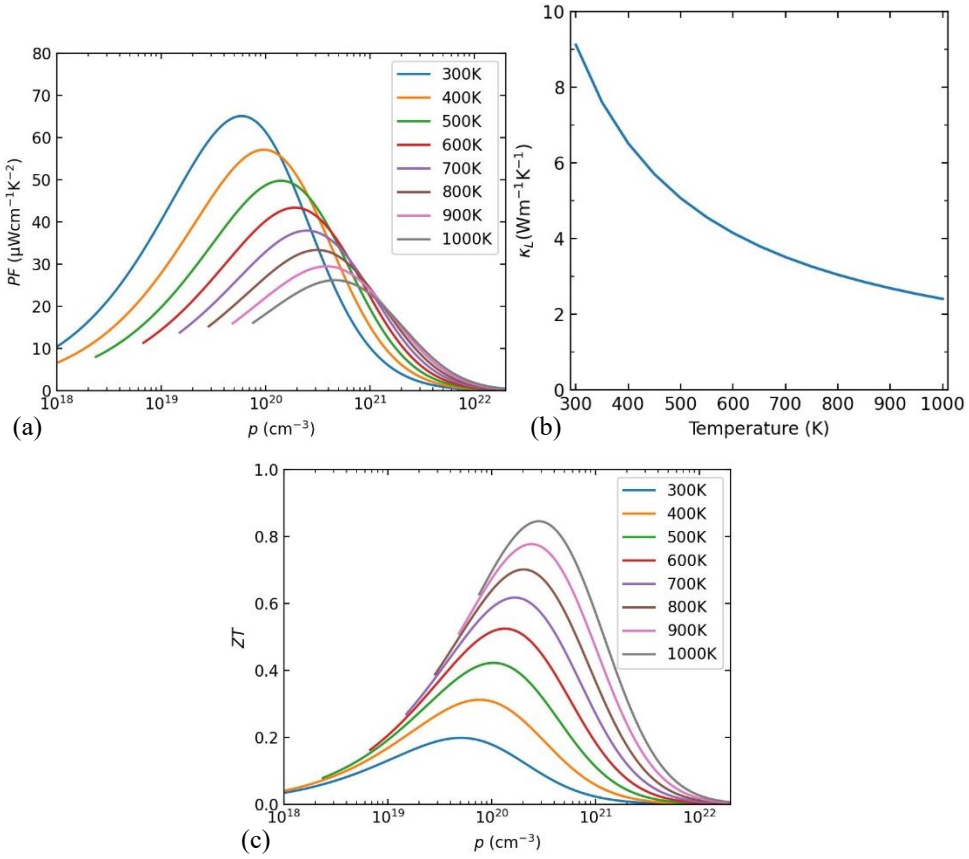

Figure S12: Thermoelectric properties of RhSbTe for *p*-type transport. (a) power factor, (b) lattice thermal conductivity, (c) figure of merit.

IrSbTe

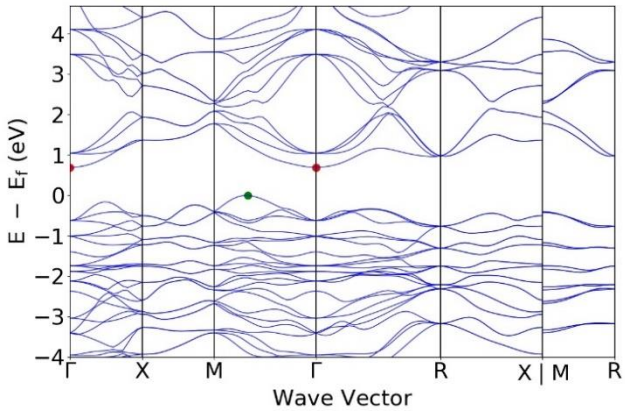

Figure S13: Band structure of IrSbTe.

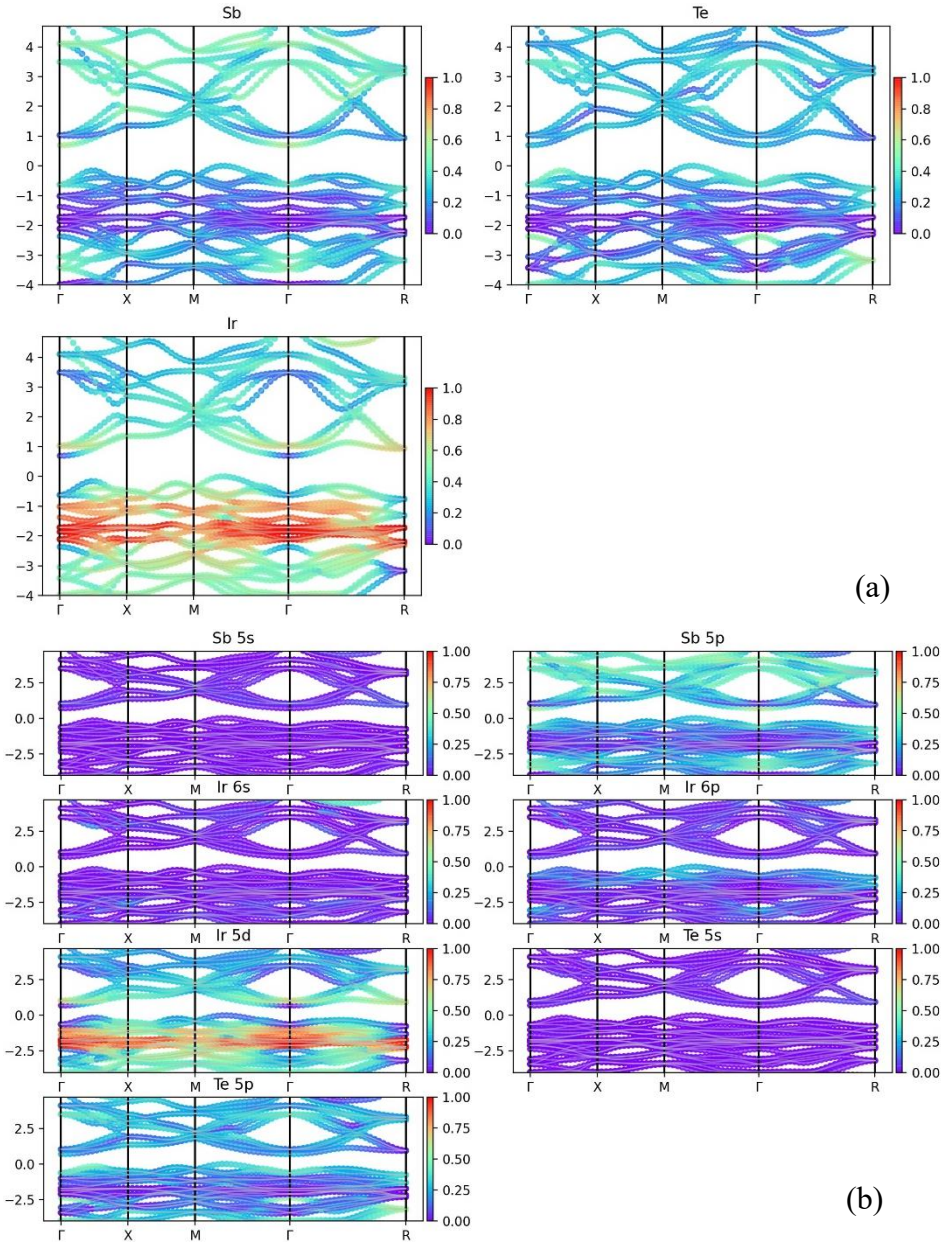

Figure S14: (a) atomic-projected and (b) orbital-projected band structure of IrSbTe.

IrBiSe

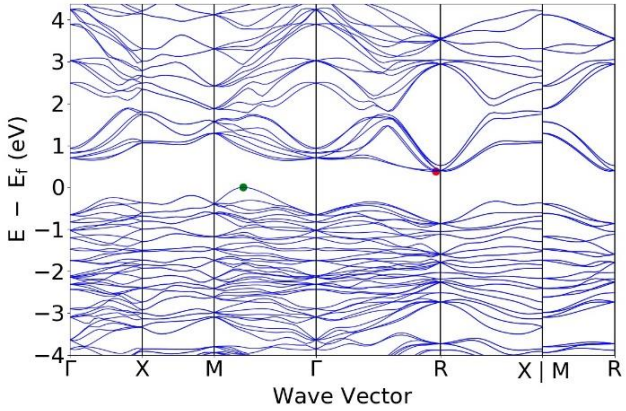

Figure S15: Band structure of IrBiSe.

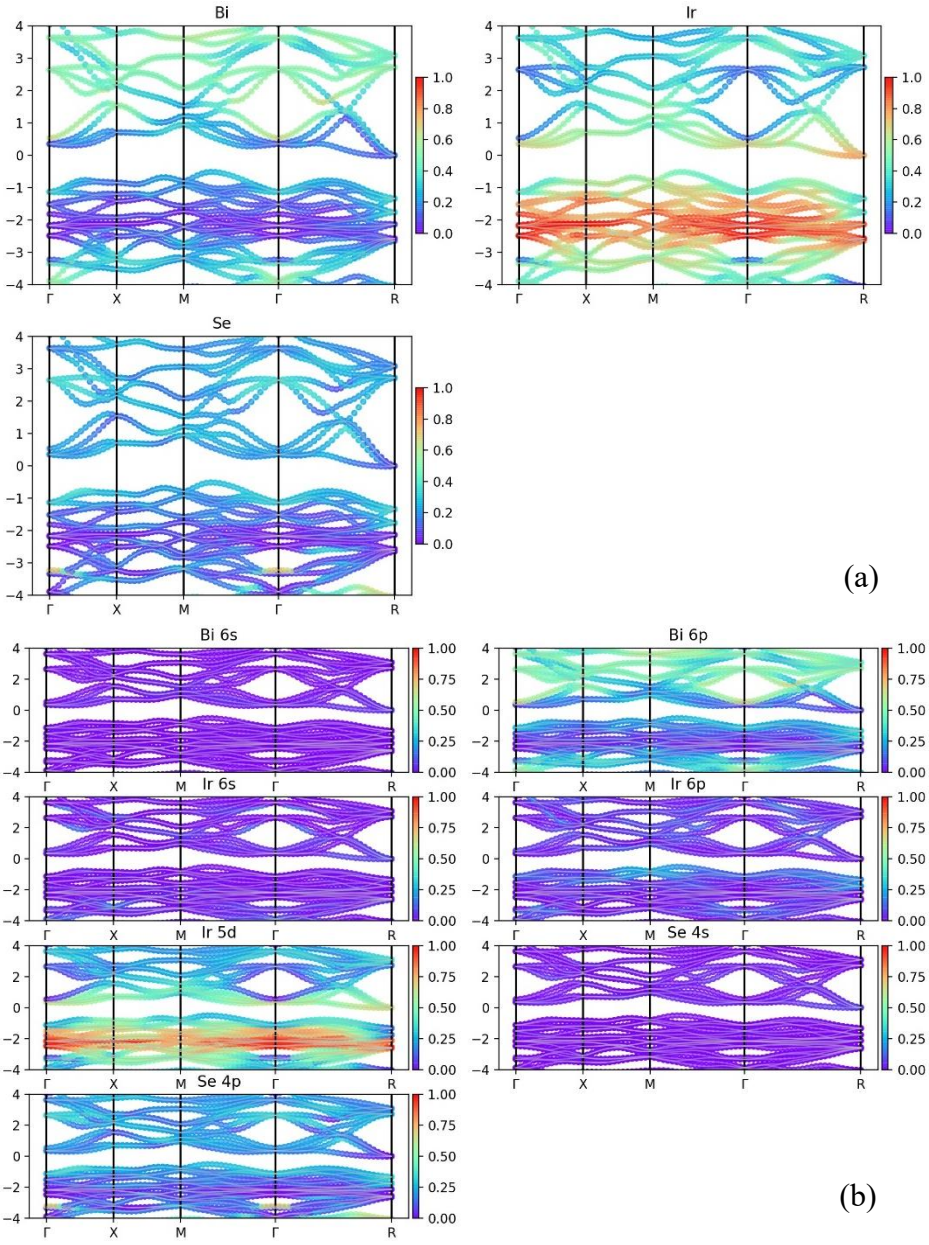

Figure S16: (a) atomic-projected and (b) orbital-projected band structure of IrBiSe.

IrBiTe

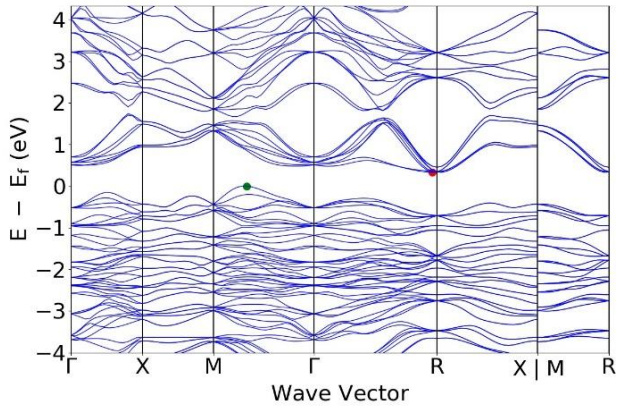

Figure S17: Band structure of IrBiTe.

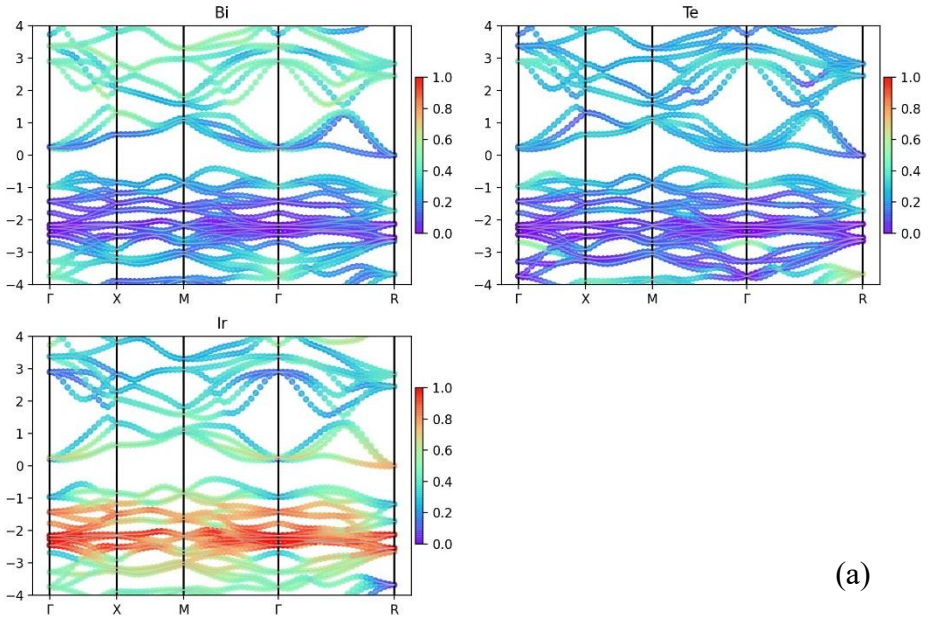

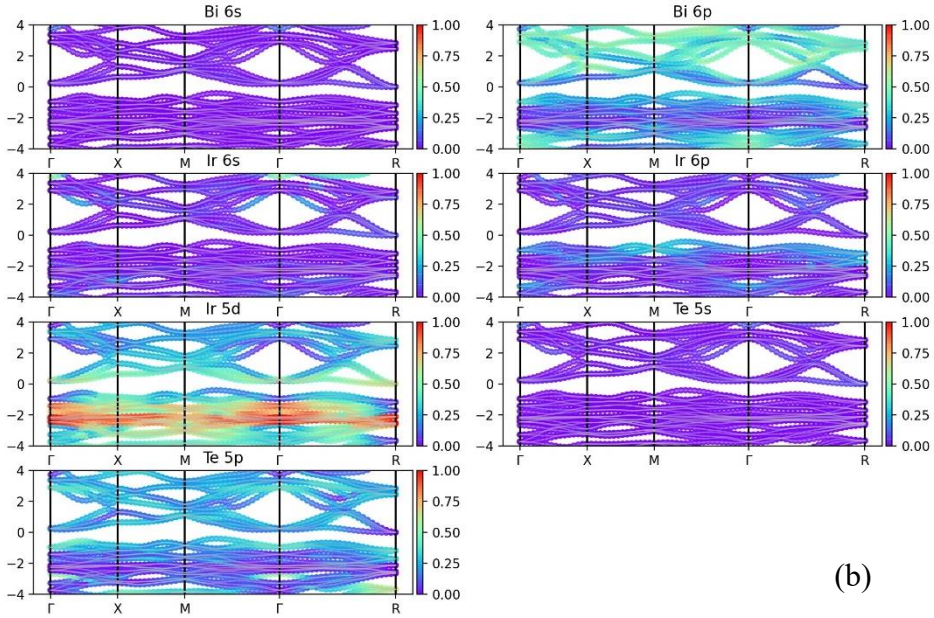

Figure S18: (a) atomic-projected and (b) orbital-projected band structure of IrBiTe.

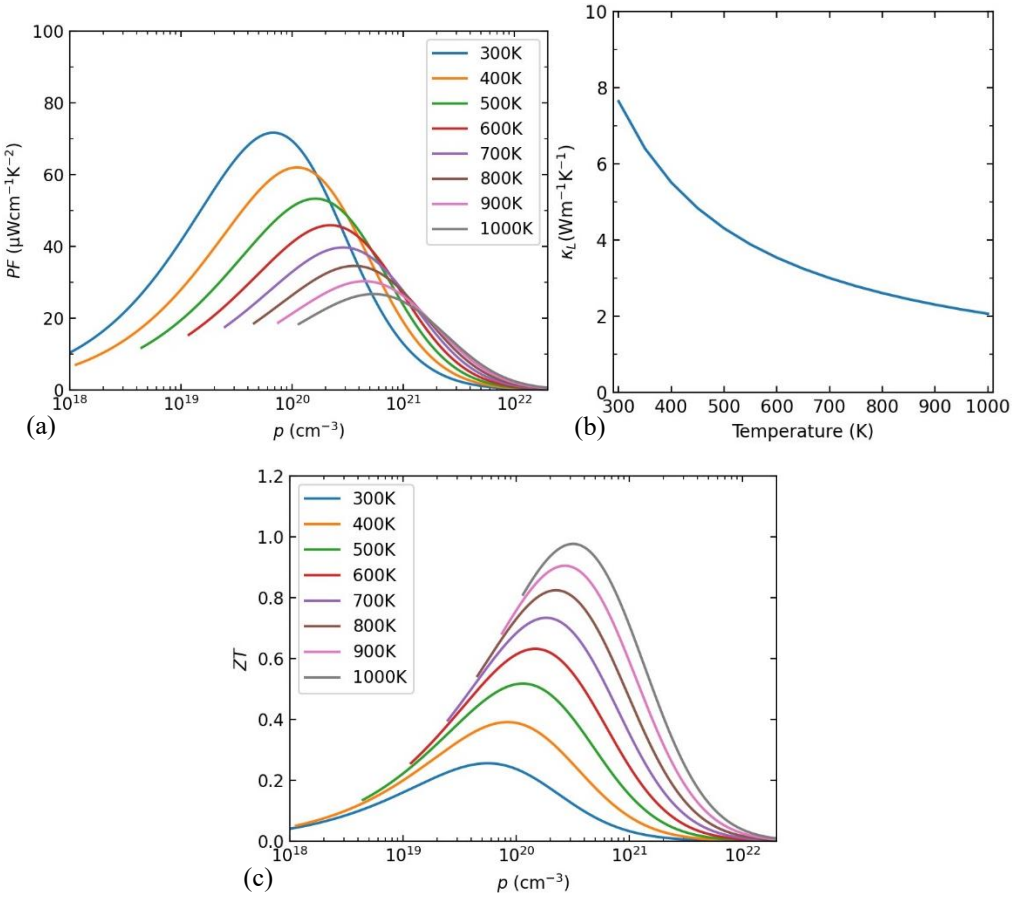

Figure S19: Thermoelectric properties of IrBiTe for *p*-type transport. (a) power factor, (b) lattice thermal conductivity, (c) figure of merit.

RhBiSe

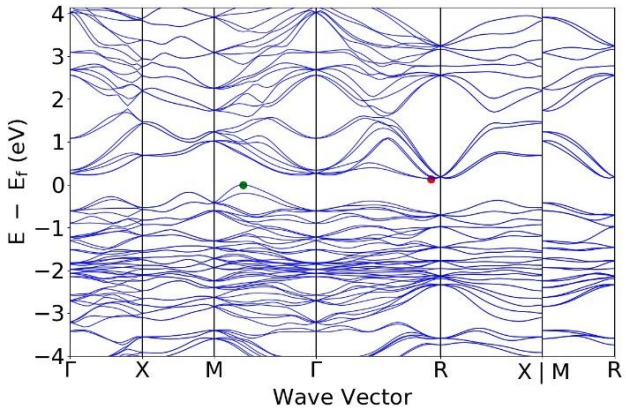

Figure S20: Band structure of RhBiSe.

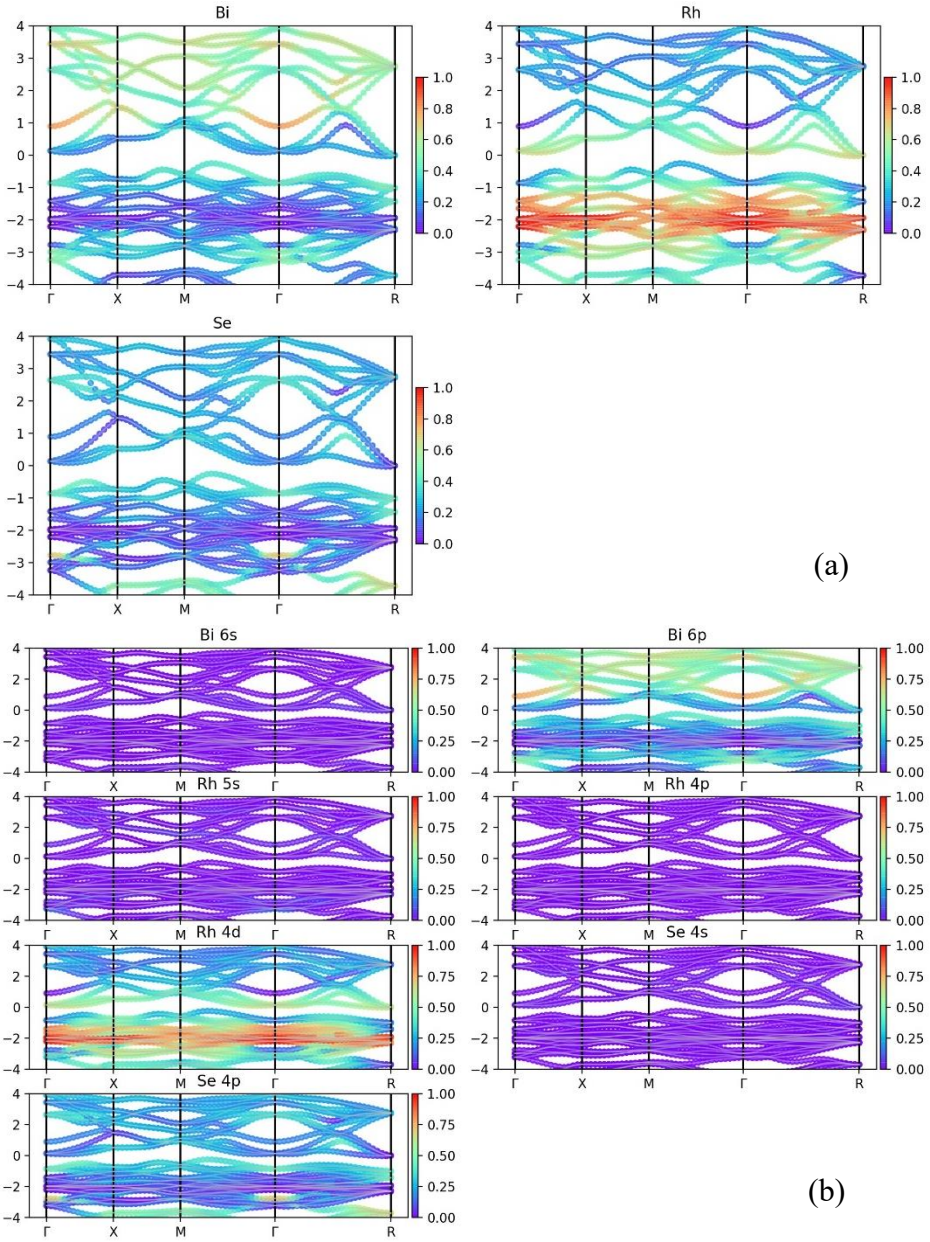

Figure S21: (a) atomic-projected and (b) orbital-projected band structure of RhBiSe.

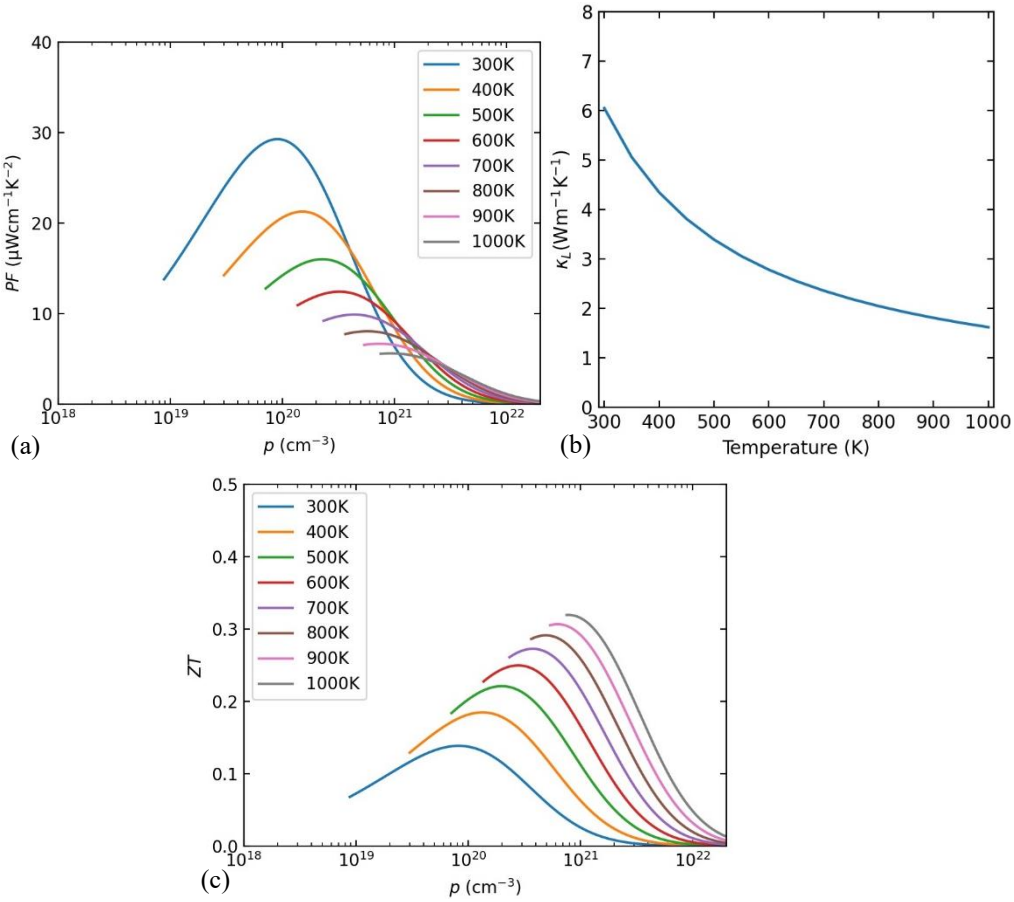

Figure S22: Thermoelectric properties of RhBiSe for *p*-type transport. (a) power factor, (b) lattice thermal conductivity, (c) figure of merit.

RhBiTe

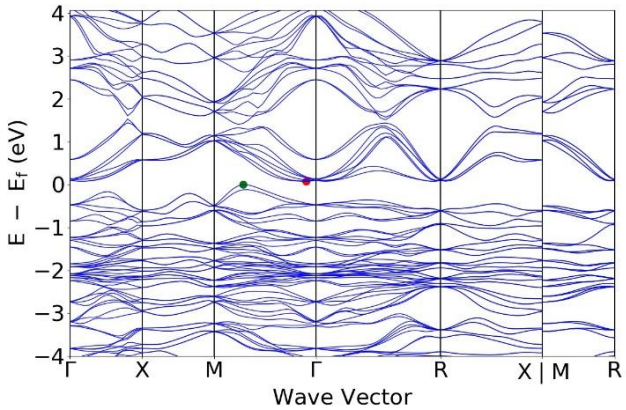

Figure S23: Band structure of RhBiTe.

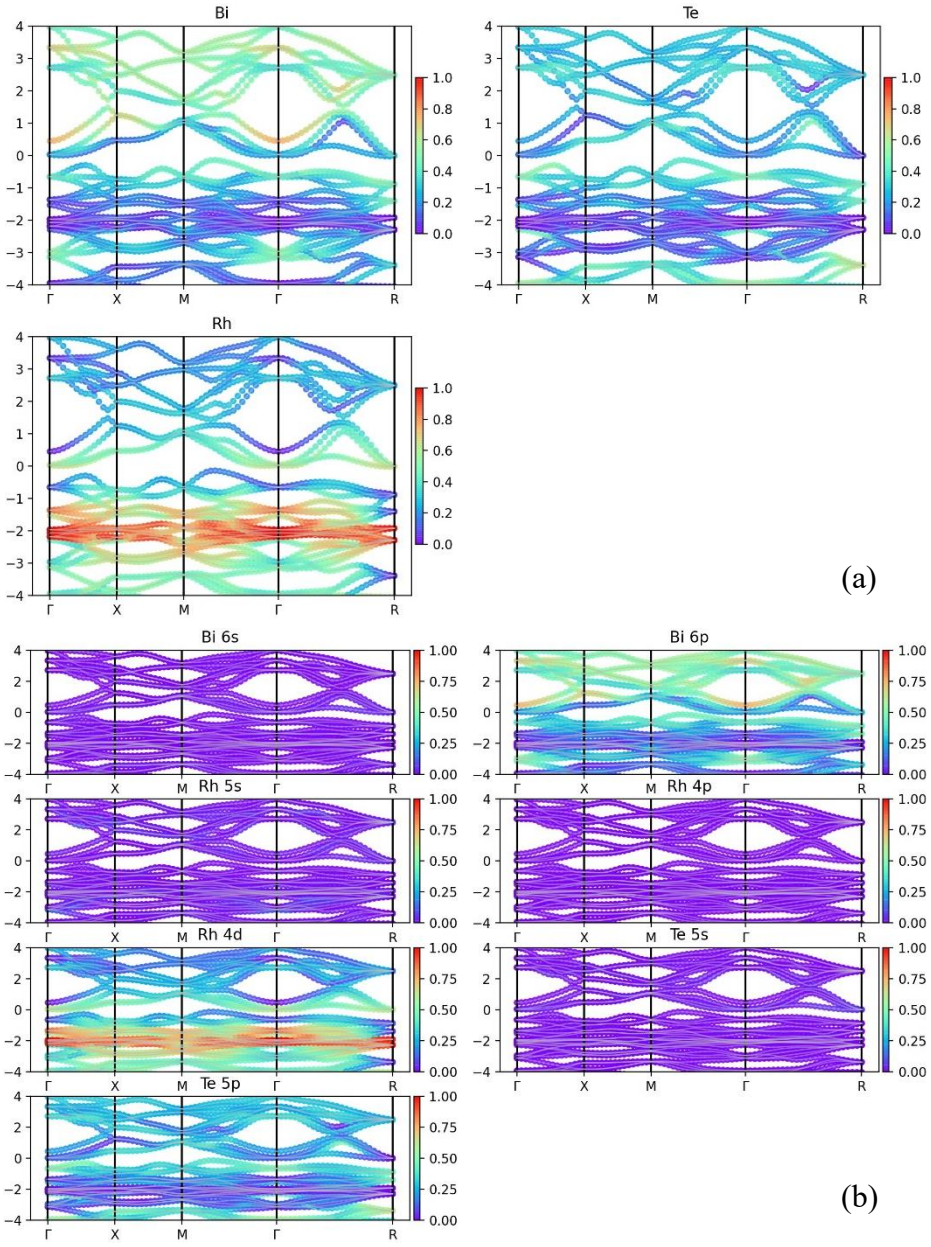

Figure S24: (a) atomic-projected and (b) orbital-projected band structure of RhBiTe.

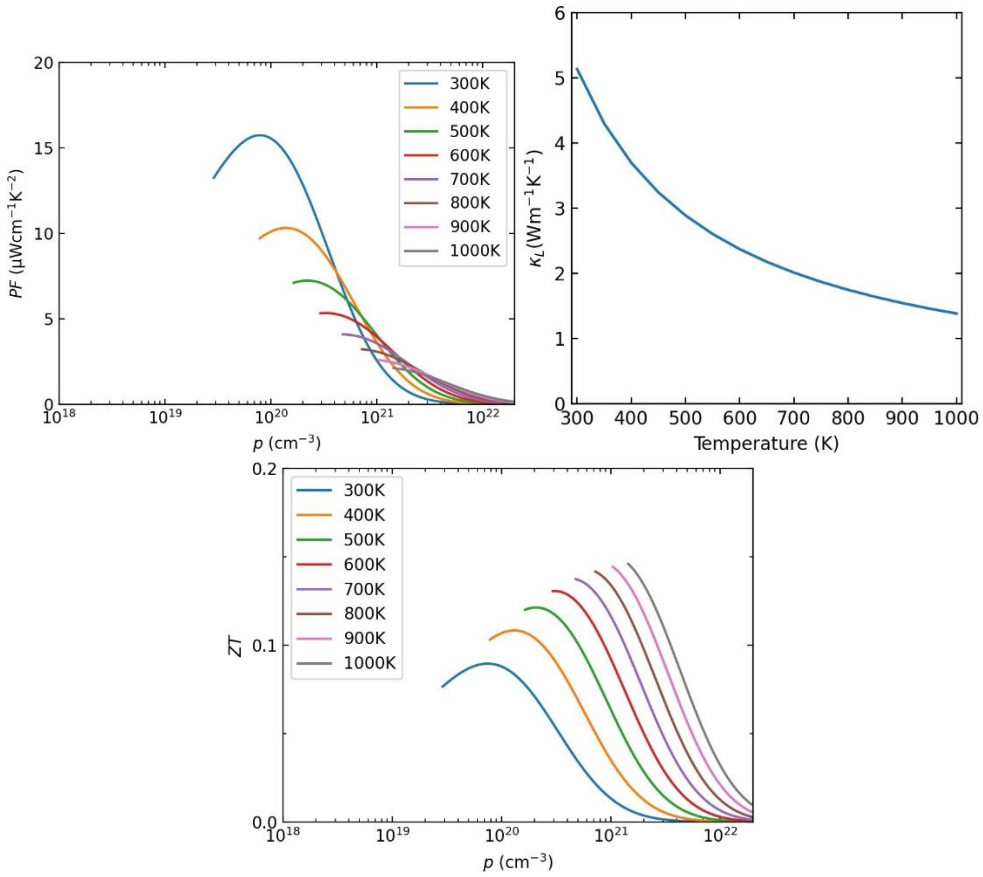

Figure S25: Thermoelectric properties of RhBiTe for *p*-type transport. (a) power factor, (b) lattice thermal conductivity, (c) figure of merit.

RhPSe

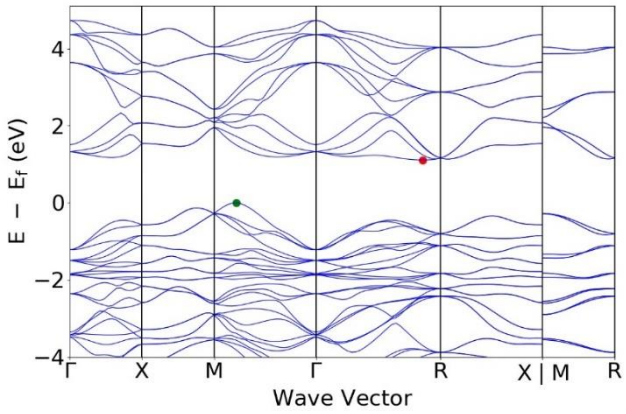

Figure S26: Band structure of RhPSe.

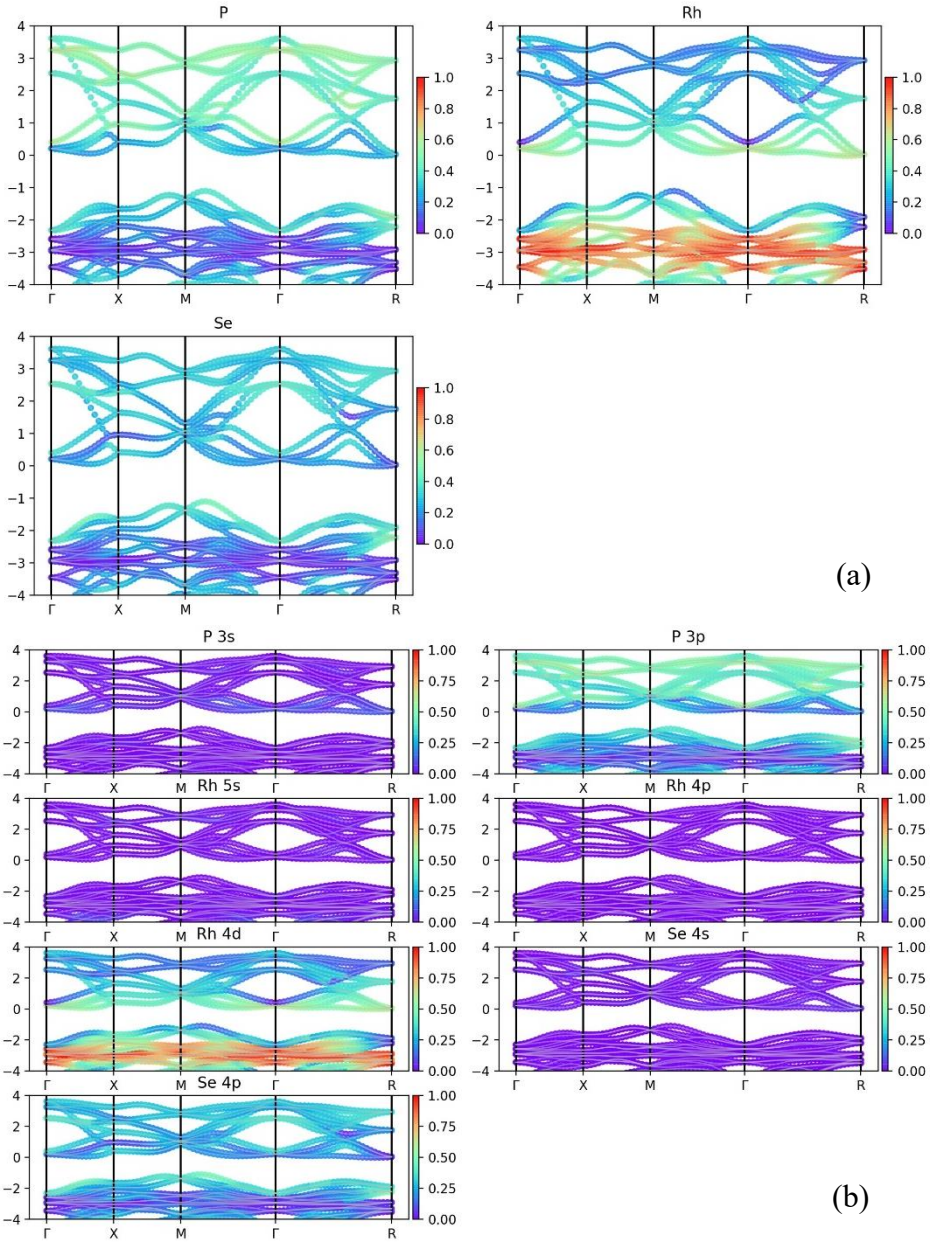

Figure S27: (a) atomic-projected and (b) orbital-projected band structure of RhPSe.

PtSnSe

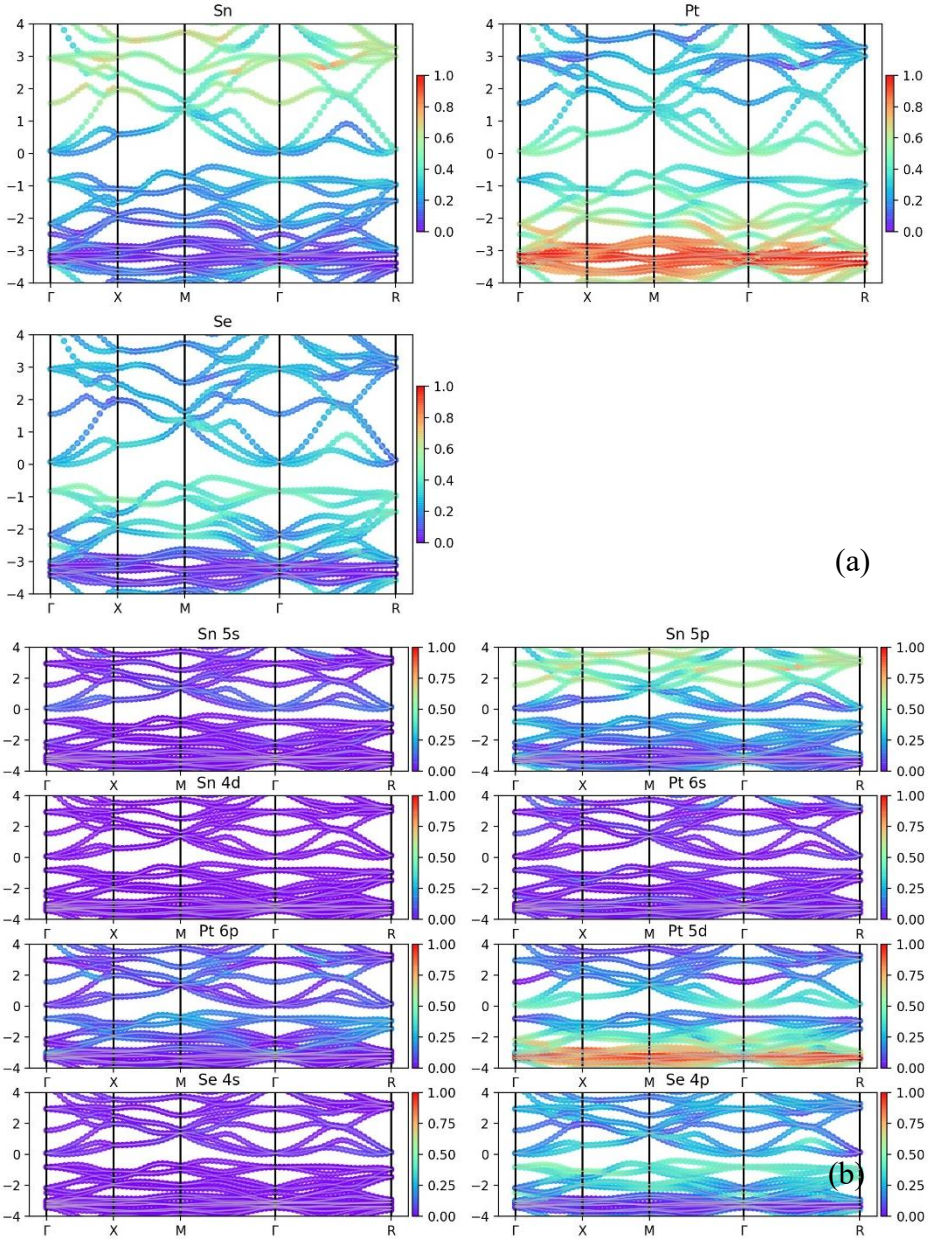

Figure S28: (a) atomic-projected and (b) orbital-projected band structure of PtSnSe.

PtGeTe

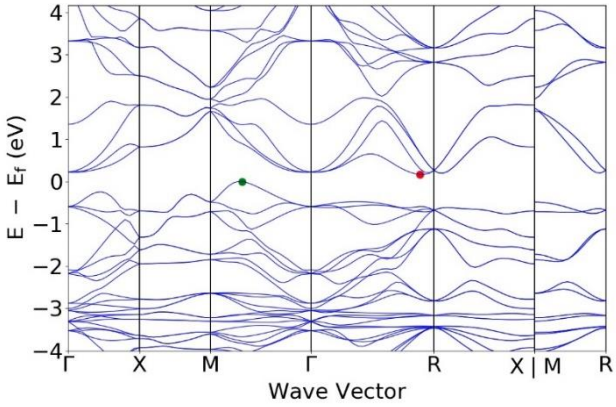

Figure S29: Band structure of PtGeTe.

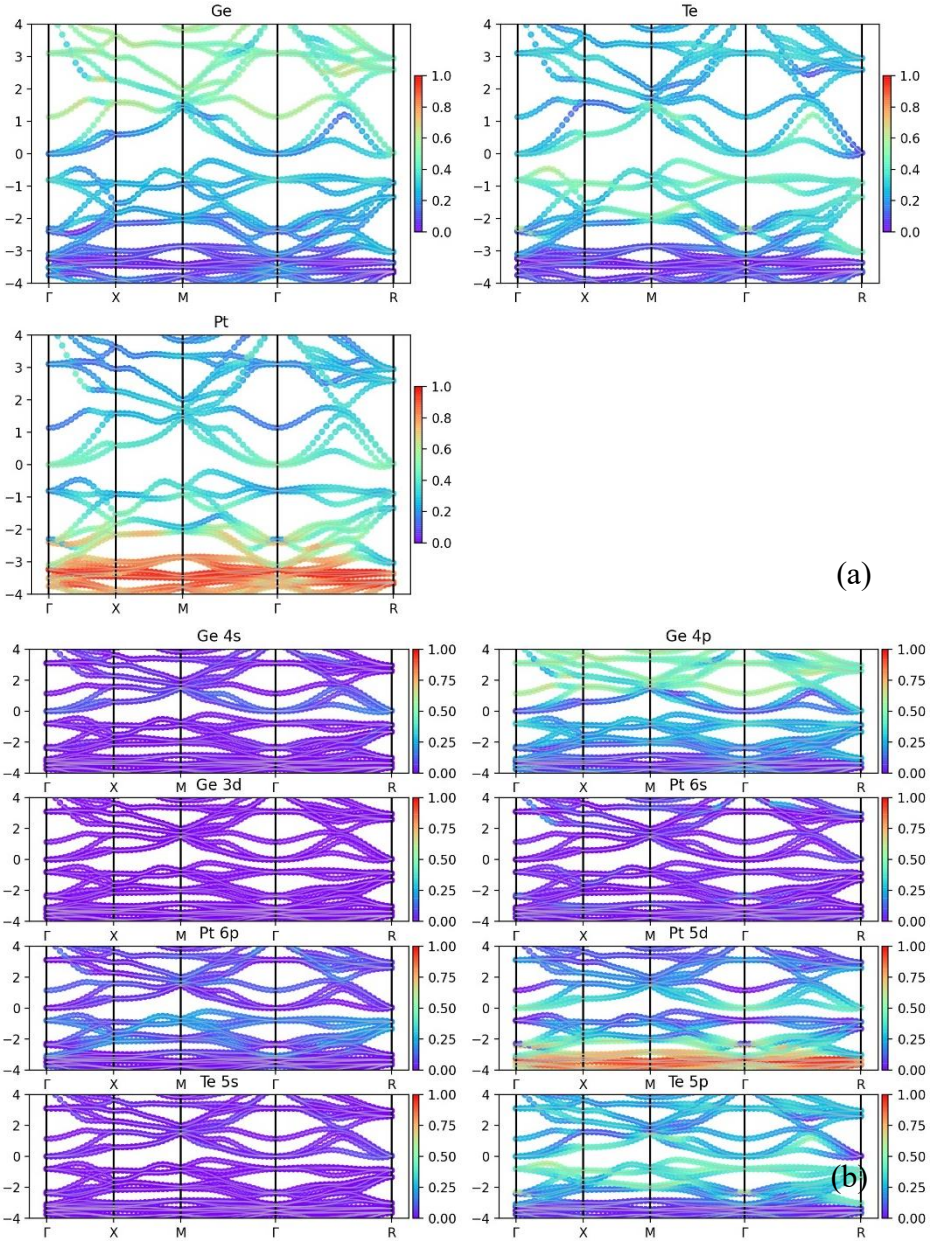

Figure S30: (a) atomic-projected and (b) orbital-projected band structure of PtGeTe.

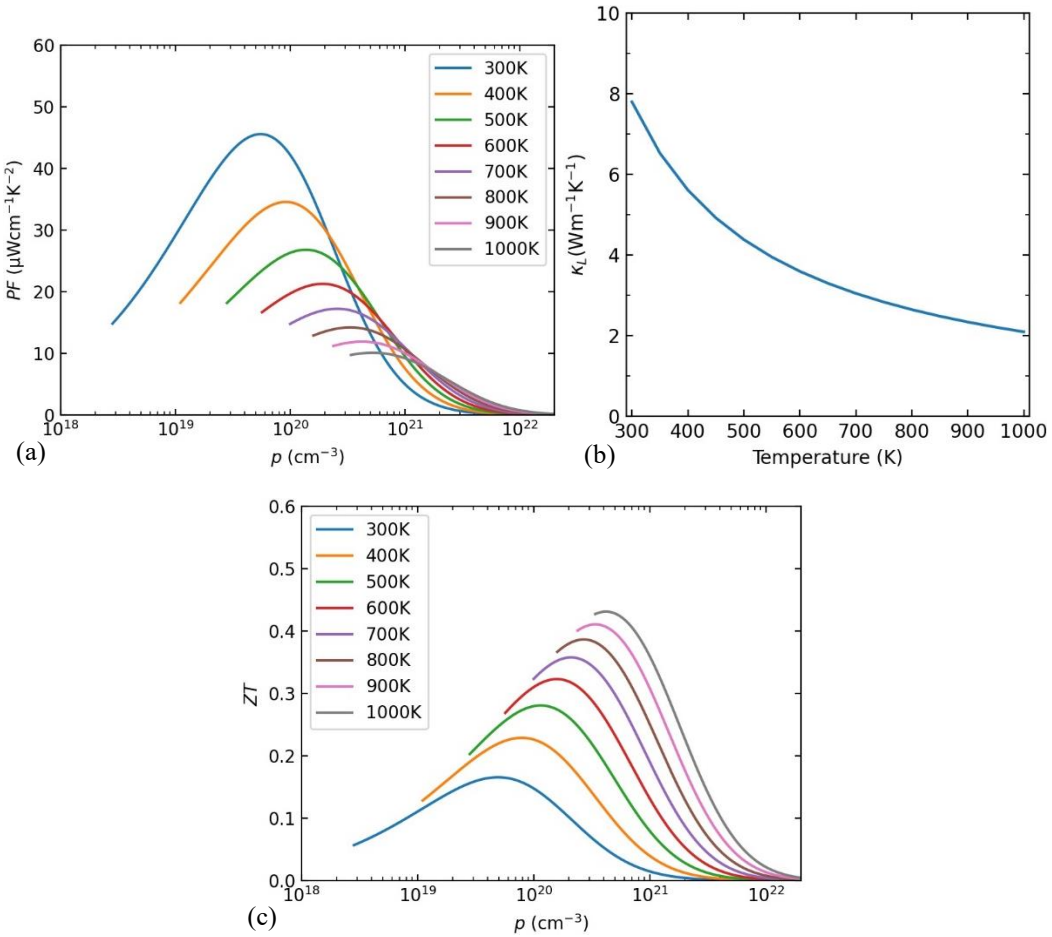

Figure S31: Thermoelectric properties of PtGeTe for *p*-type transport. (a) power factor, (b) lattice thermal conductivity, (c) figure of merit.

2. CdSe2

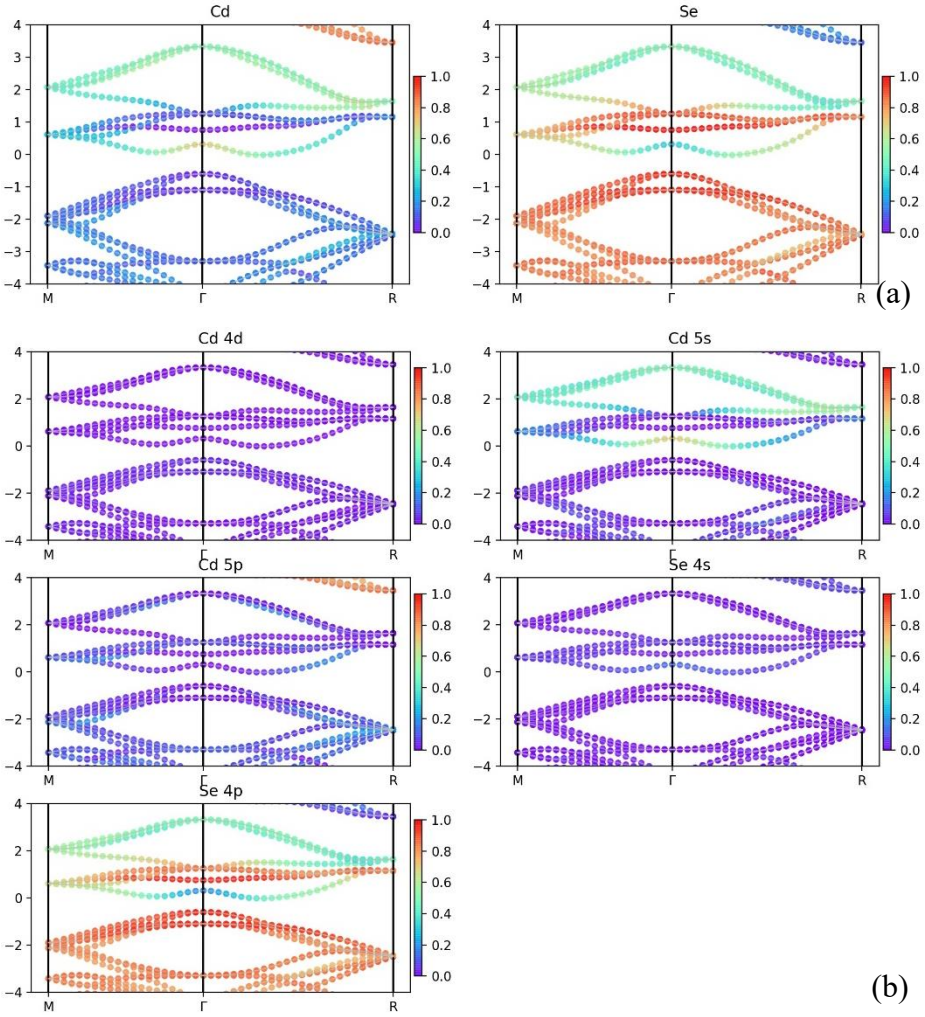

Figure S32: (a) atomic-projected and (b) orbital-projected band structure of CdSe2.

3. $XAcTe_2$ (X = I A or III A)

Compounds with this chemical formula include $NaAcTe_2$, $KAcTe_2$, $RbAcTe_2$, $CsAcTe_2$, $GaAcTe_2$, $InAcTe_2$ and $TlAcTe_2$. These compounds share the same structure (space group *F*m-3m), as shown in Fig. S33. According to our calculation, this group of compounds have very high figure of merit values, mainly due to their relatively high power factor and extremely low lattice thermal conductivity. However, since they contain Ac element and it is a radioactive element, it is unpractical to really manufacture devices based on these compounds.

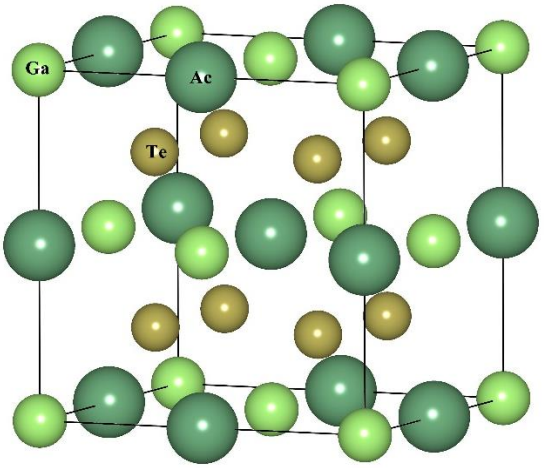

Figure S33: Crystal structure of GaAcTe2.

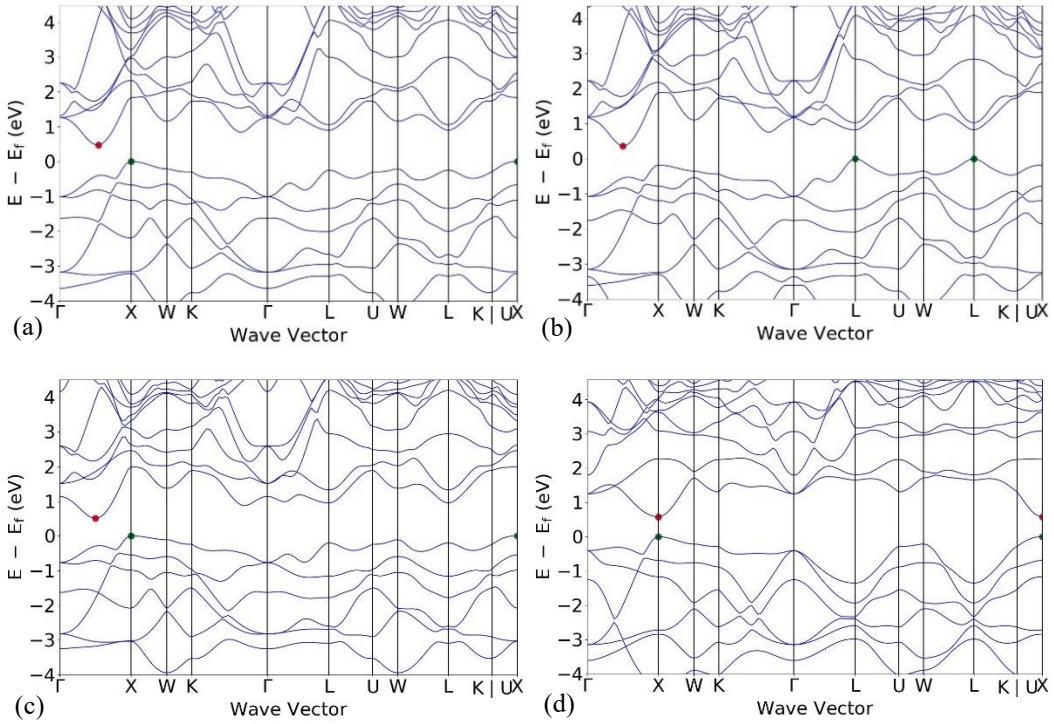

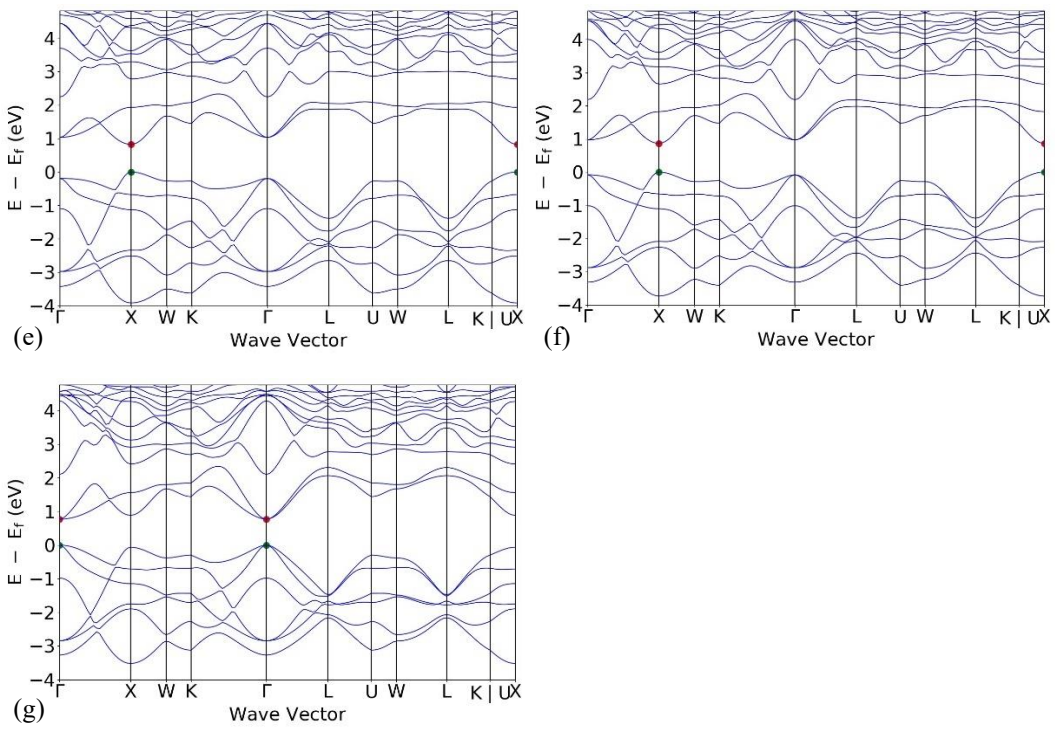

Figure S34: Band structures of (a) $GaAcTe_2$, (b) $InAcTe_2$, (c) $TlAcTe_2$, (d) $NaAcTe_2$, (e) $KAcTe_2$, (f) $RbAcTe_2$, (g) $CsAcTe_2$.

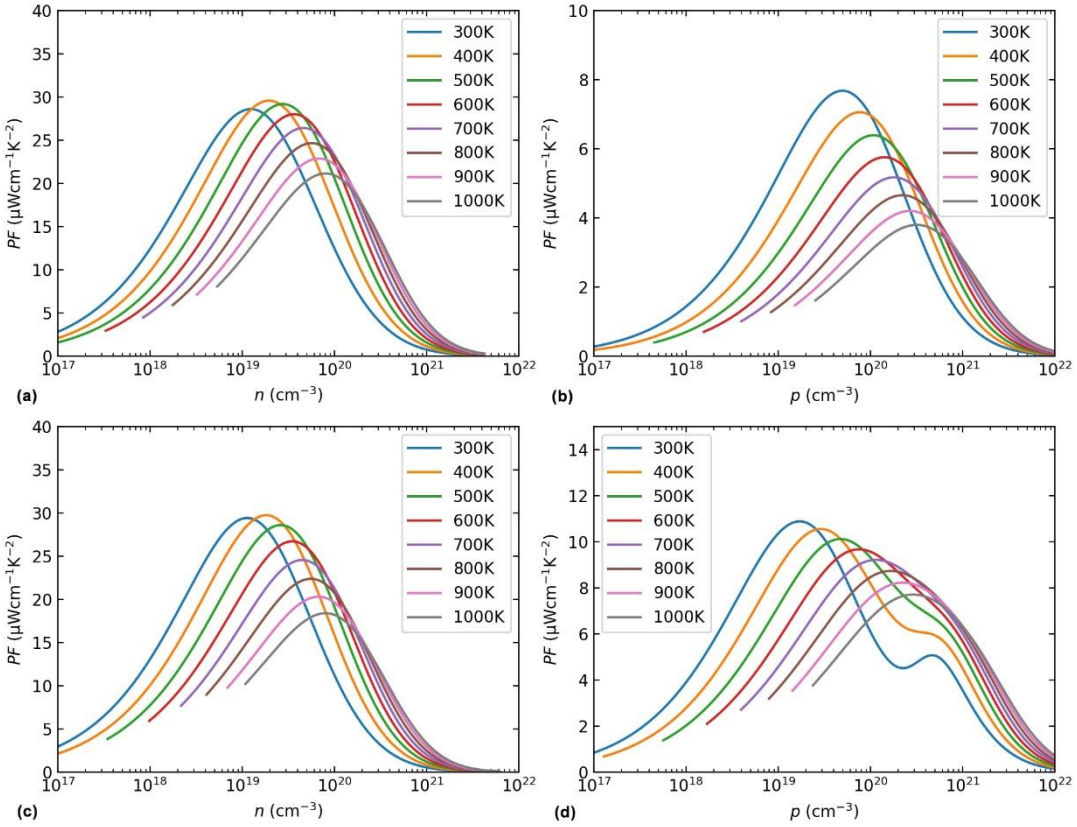

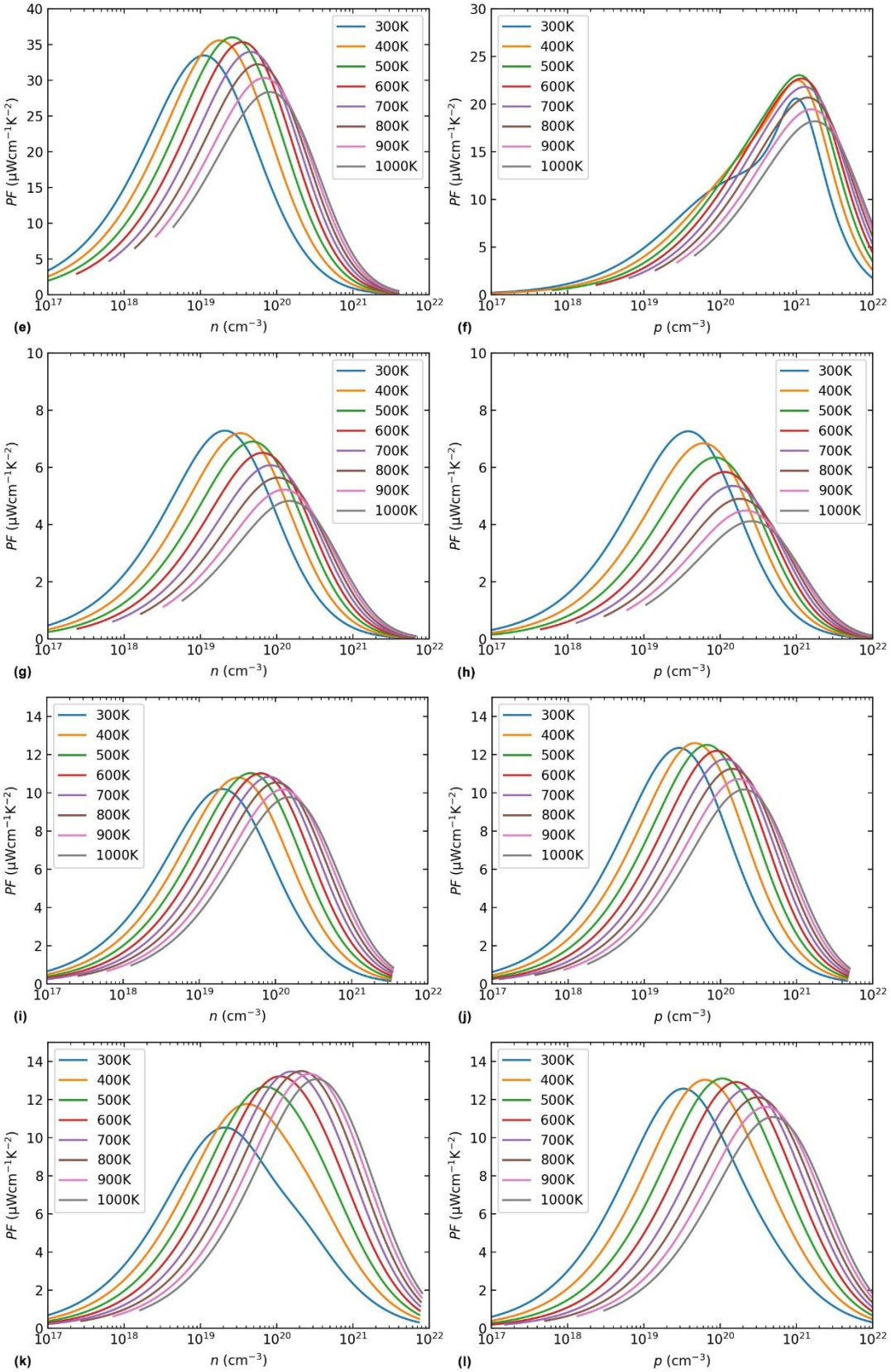
(e)
(f)
(g)
(h)
(i)
(j)
(k)
(l)
PF (μWcm⁻¹K⁻²)
n (cm⁻³)
p (cm⁻³)
300K
400K
500K
600K
700K
800K
900K
1000K

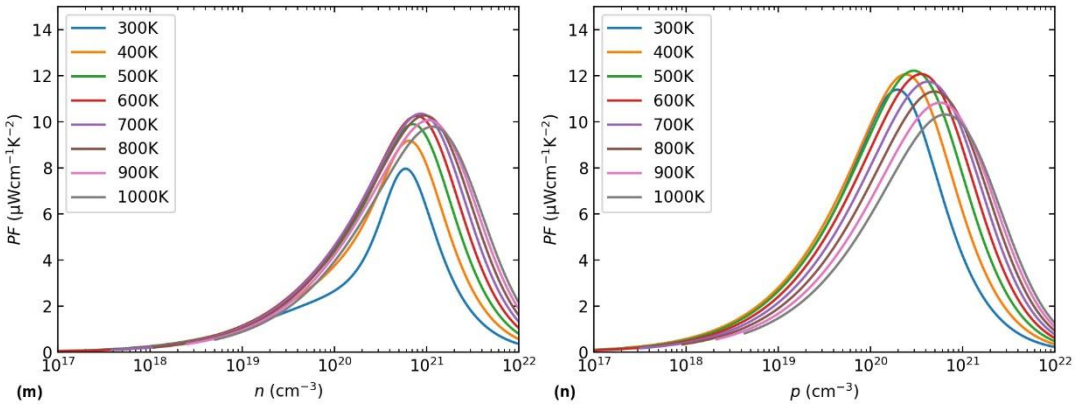

Figure S35: Power factors at varying temperatures and carrier concentrations for (a)(b) $GaAcTe_2$, (c)(d) $InAcTe_2$, (e)(f) $TlAcTe_2$, (g)(h) $NaAcTe_2$, (i)(j) $KAcTe_2$, (k)(l) $RbAcTe_2$, (m)(n) $CsAcTe_2$.

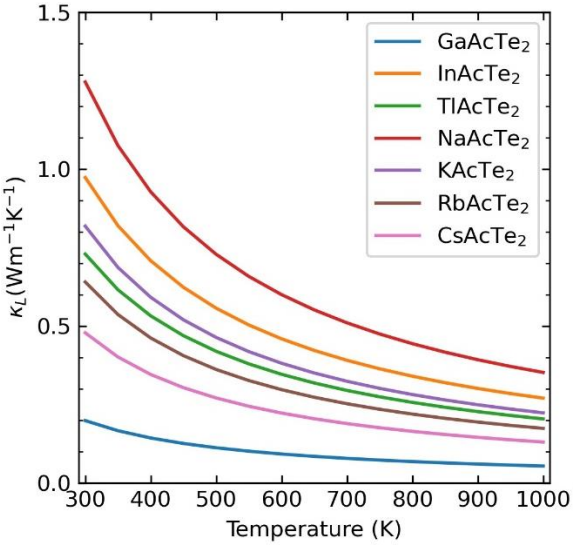

Figure S36: Lattice thermal conductivity of this group of compounds.

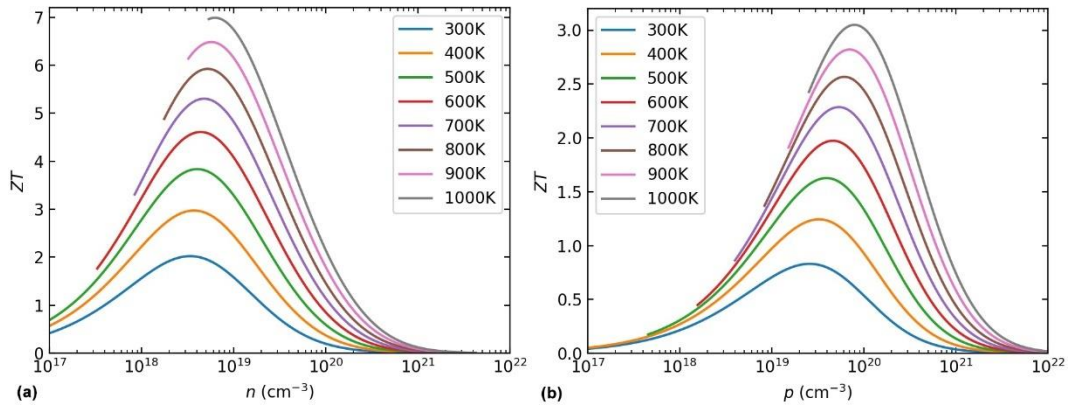

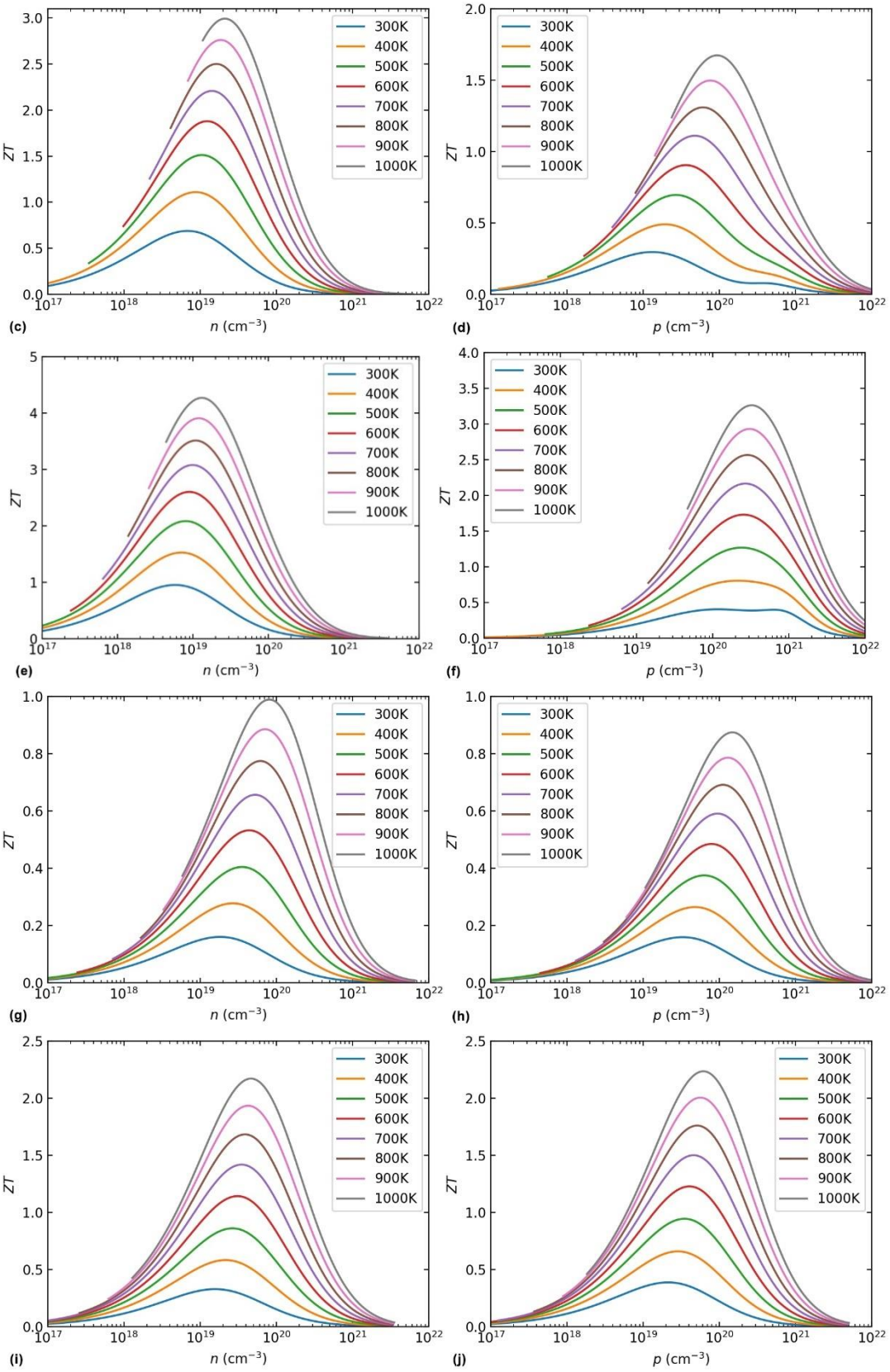
(c)
(d)
(e)
(f)
(g)
(h)
(i)
(j)
ZT
n (cm⁻³)
p (cm⁻³)
300K
400K
500K
600K
700K
800K
900K
1000K

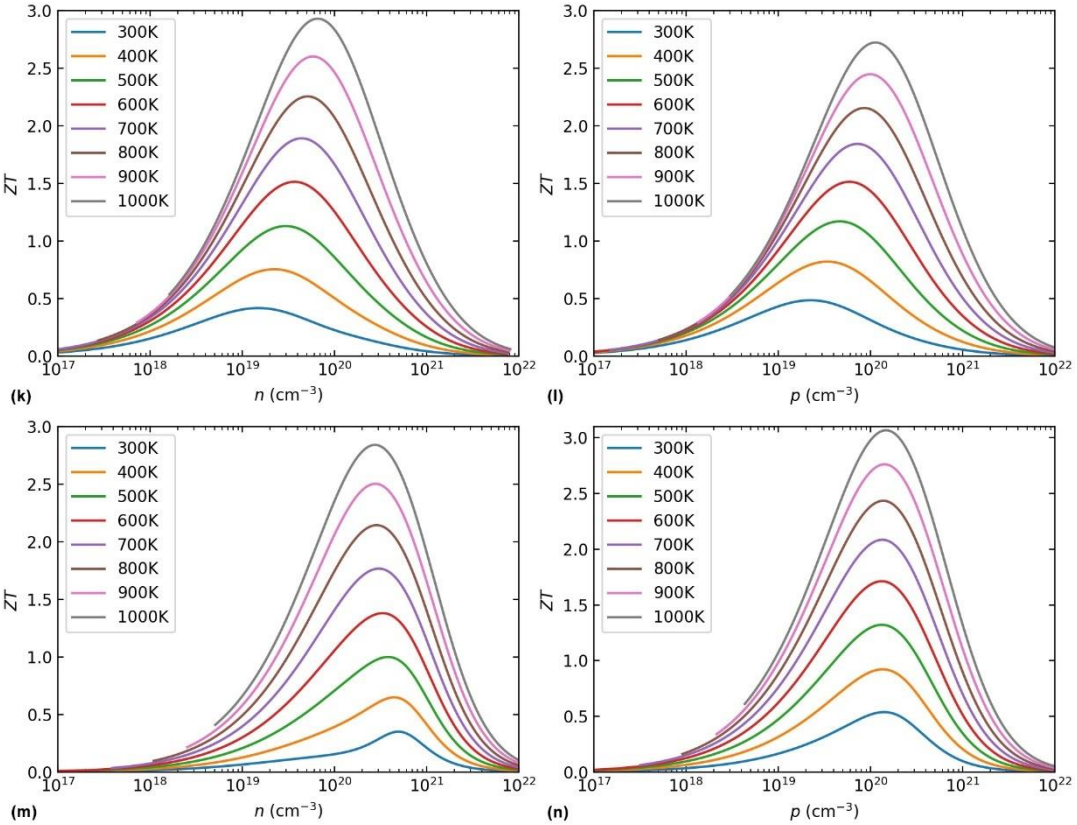

Figure S37: Figure of merit at varying temperatures and carrier concentrations for (a)(b) $GaAcTe_2$, (c)(d) $InAcTe_2$, (e)(f) $TlAcTe_2$, (g)(h) $NaAcTe_2$, (i)(j) $KAcTe_2$, (k)(l) $RbAcTe_2$, (m)(n) $CsAcTe_2$.

4. X_4Y_8 (X = VIII B, Y = VI A)

Compounds with this chemical formula include Fe_4S_8, Ru_4S_8, Ru_4Se_8, $Ru_4Se_4S_4$. These compounds share the same structure (space group *P*a-3), as shown in Fig. S38. Each VIII B atom form an octahedron with six VI A atoms. According to our calculation, this group of compounds could have high power factor for *p*-type transport. The main problem is their lattice thermal conductivity could also be high. Thus, the figure of merit is not good.

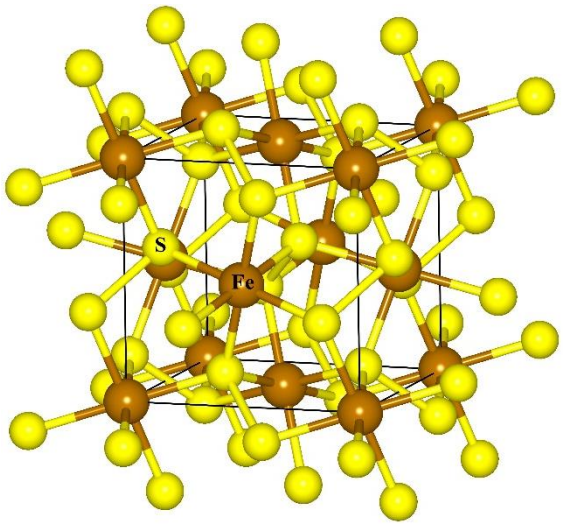

Figure S38: Crystal structure of Fe_4S_8.

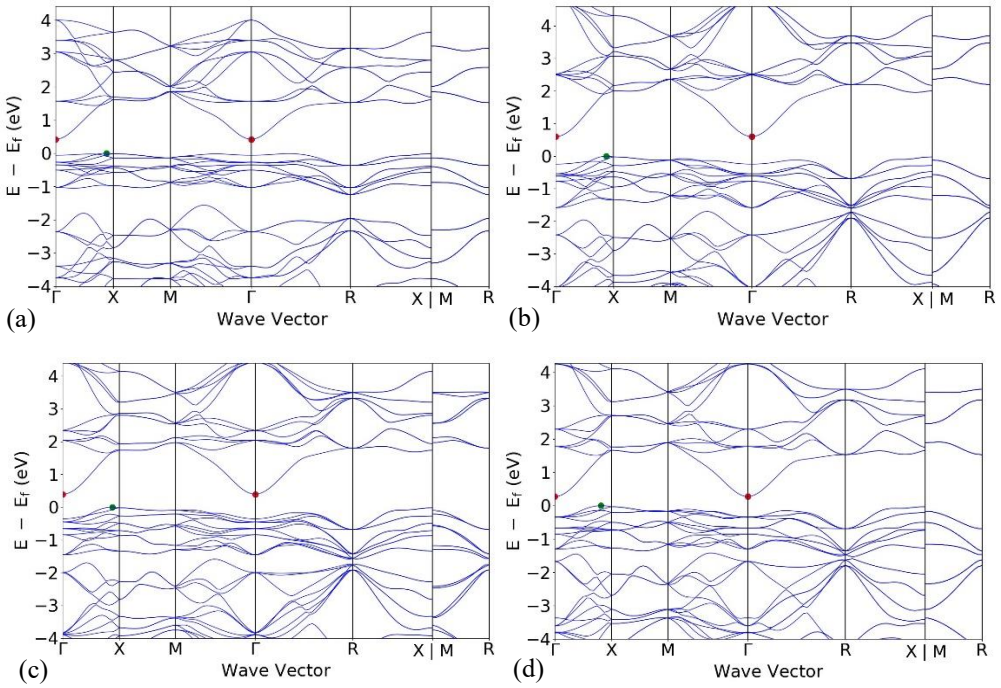

Figure S39: Band structures of (a) Fe_4S_8, (b) Ru_4S_8, (c) $Ru_4Se_4S_4$, (d) Ru_4Se_8.

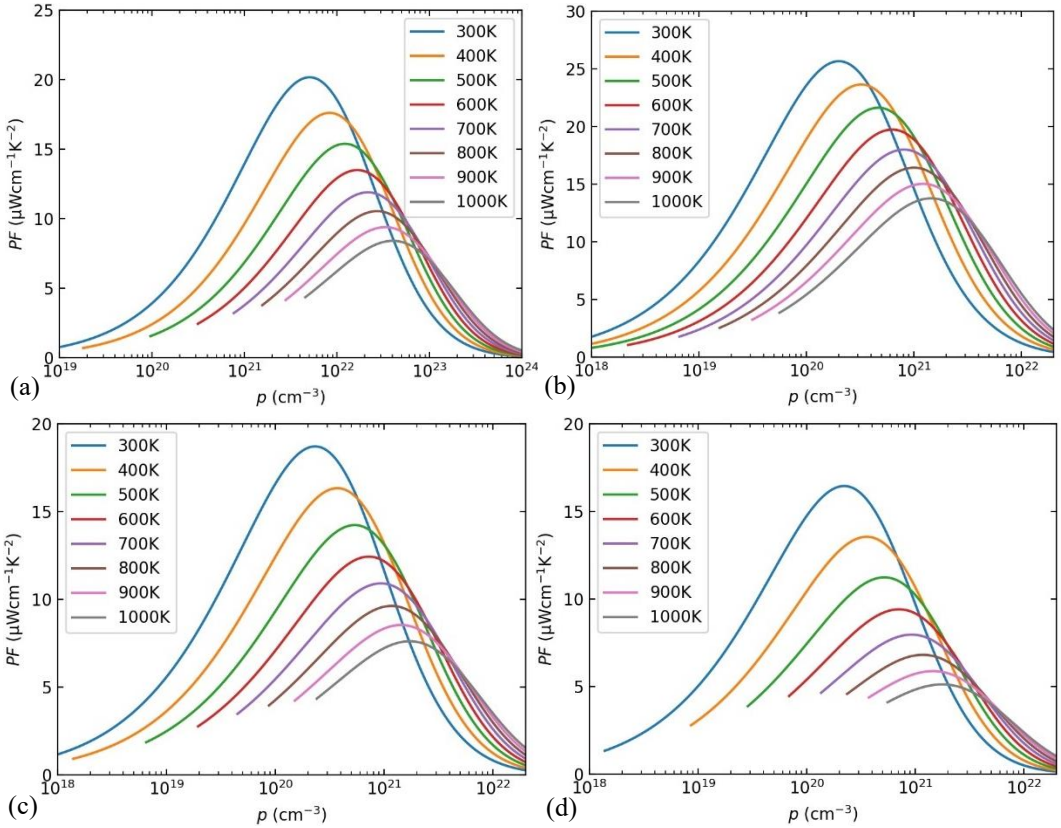

Figure S40: Power factors at varying temperatures and carrier concentrations for (a) Fe_4S_8, (b) Ru_4S_8, (c) $Ru_4Se_4S_4$, (d) Ru_4Se_8.

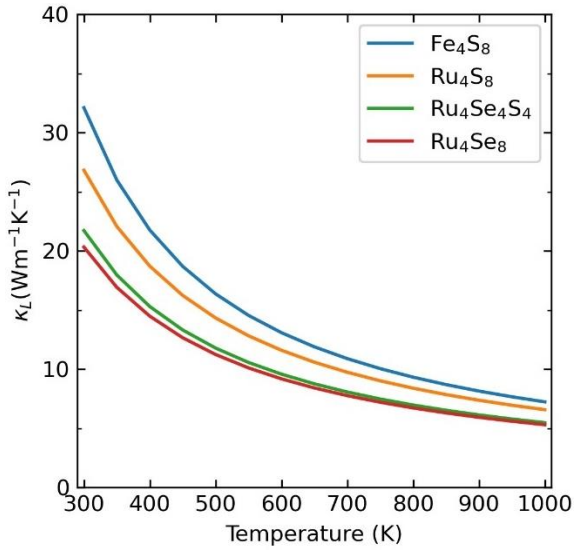

Figure S41: Lattice thermal conductivity of this group of compounds.

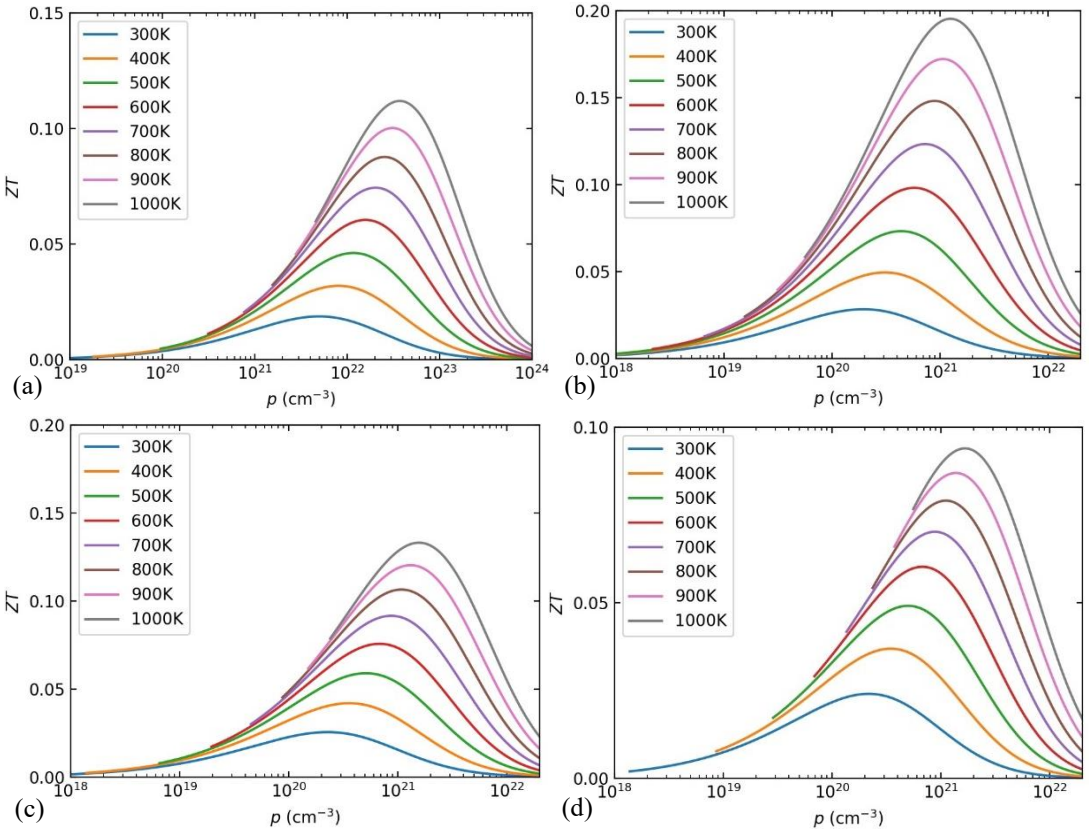

Figure S42: Figure of merit at varying temperatures and carrier concentrations for (a) Fe_4S_8, (b) Ru_4S_8, (c) $Ru_4Se_4S_4$, (d) Ru_4Se_8.

5. $X_2Y_4Z_8$ (X = II B, Y = III A, Z = VI A)

Compounds with this chemical formula include $Hg_2Al_4Se_8$, $Cd_2In_4Se_4S_4$, $Hg_2In_4S_8$. These compounds share the same structure (space group *F*d-3m), as shown in Fig. S43. Each III A atom forms a distorted octahedron with six VI A atoms, while each II B atom forms a tetrahedron with four VI A atoms. According to our calculation, this group of compounds could have high power factor for *p*-type transport and their lattice thermal conductivity are relatively low. Therefore, the figure of merit could be above 1 at high temperature.

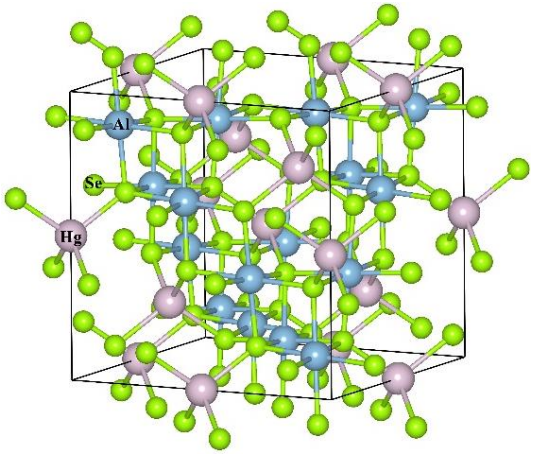

Figure S43: Crystal structure of $Hg_2Al_4Se_8$.

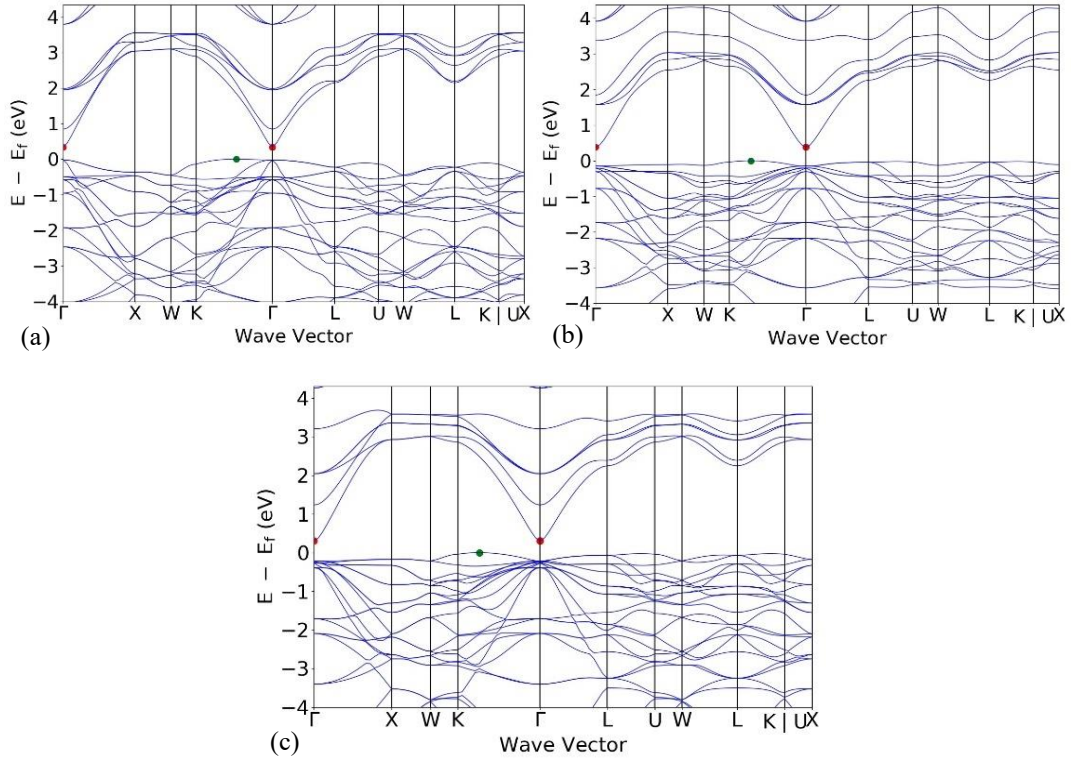

Figure S44: Band structures of (a) $Hg_2Al_4Se_8$, (b) $Cd_2In_4Se_4S_4$, (c) $Hg_2In_4S_8$.

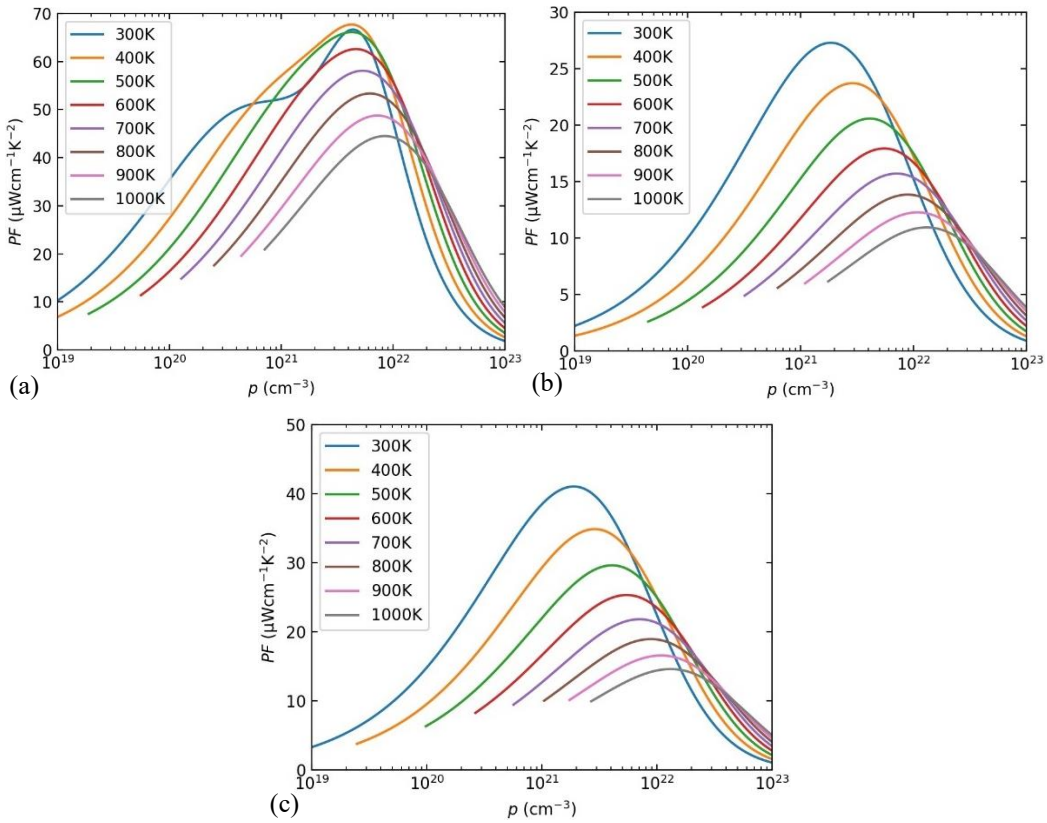

Figure S45: Power factor at varying temperatures and carrier concentrations for (a) $Hg_2Al_4Se_8$, (b) $Cd_2In_4Se_4S_4$, (c) $Hg_2In_4S_8$.

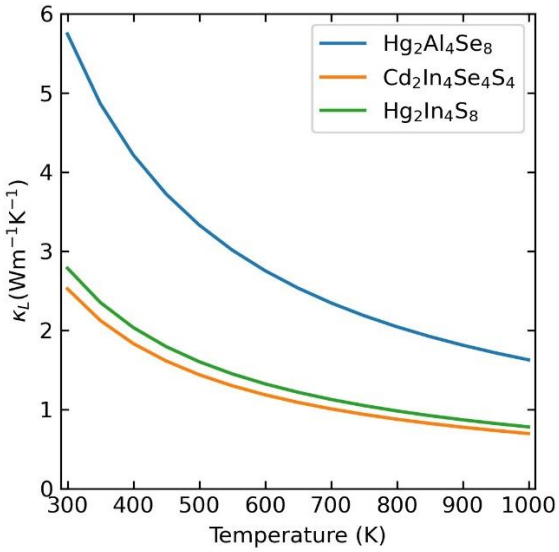

Figure S46: Lattice thermal conductivity of this group of compounds.

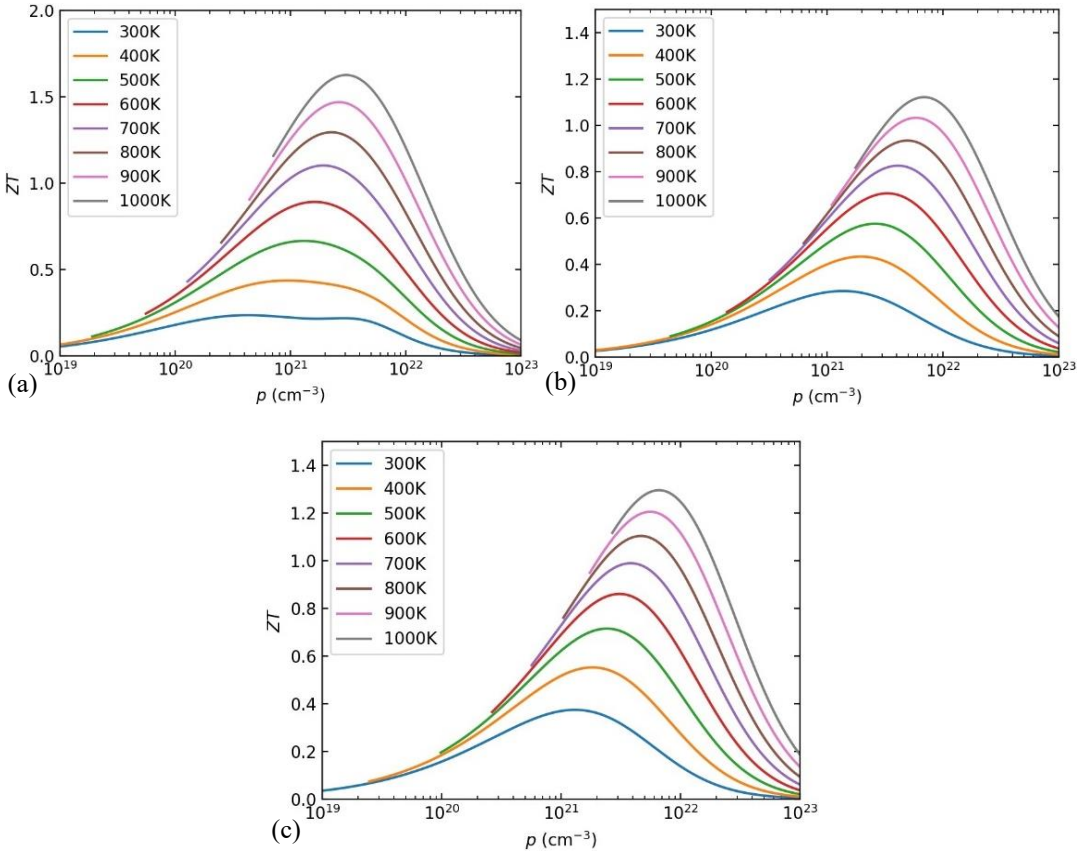

Figure S47: Figure of merit at varying temperatures and carrier concentrations for (a) $Hg_2Al_4Se_8$, (b) $Cd_2In_4Se_4S_4$, (c) $Hg_2In_4S_8$.

6. ScCoTe, TiFeTe and ZrFeTe

These three compounds have the same crystal structure (space group *F*-43m), as shown in Fig. S48. According to our calculation, this group of compounds are promising *n*-type thermoelectric materials.

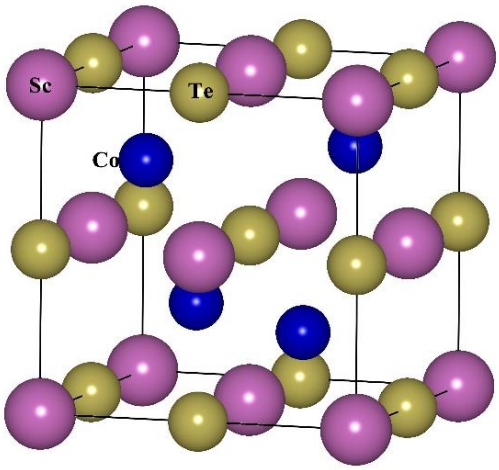

Figure S48: Crystal structure of ScCoTe.

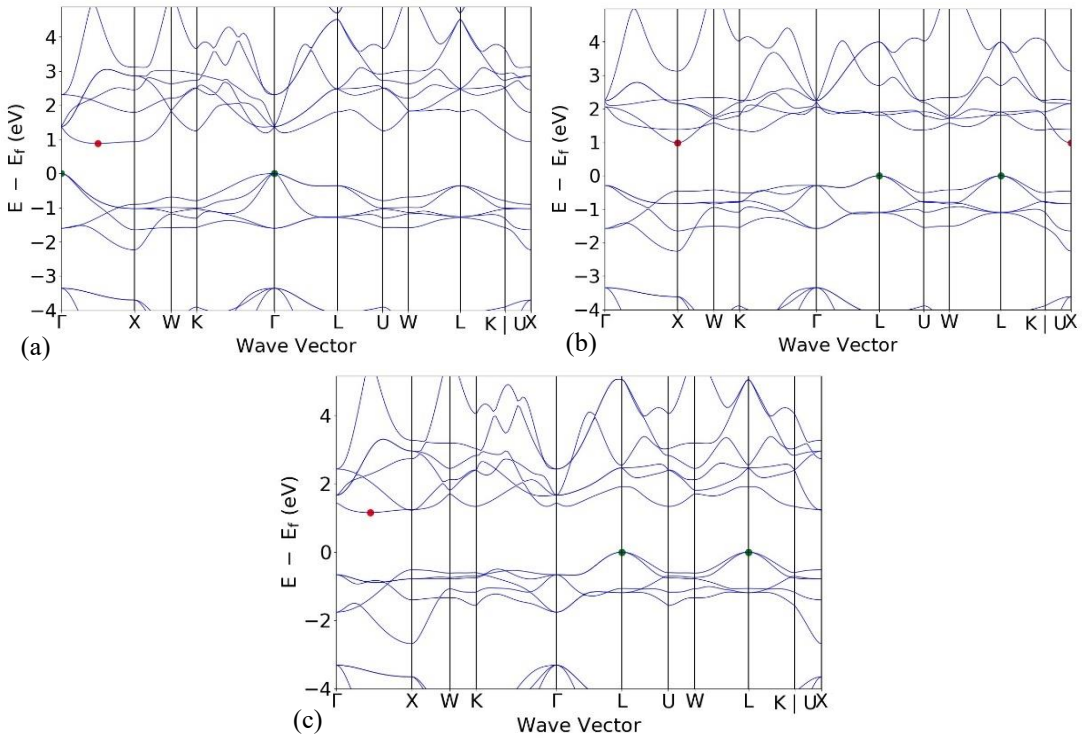

Figure S49: Band structures of (a) ScCoTe, (b) TiFeTe, (c) ZrFeTe.

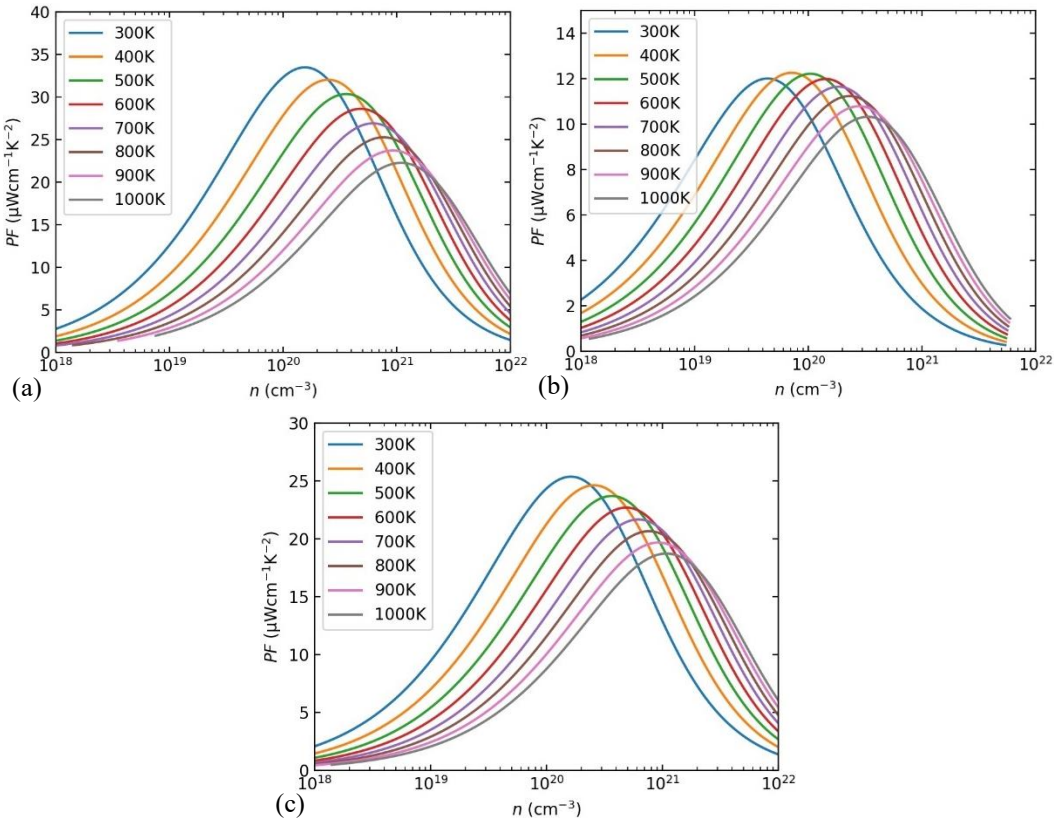

Figure S50: Power factor at varying temperatures and carrier concentrations for (a) ScCoTe, (b) TiFeTe, (c) ZrFeTe.

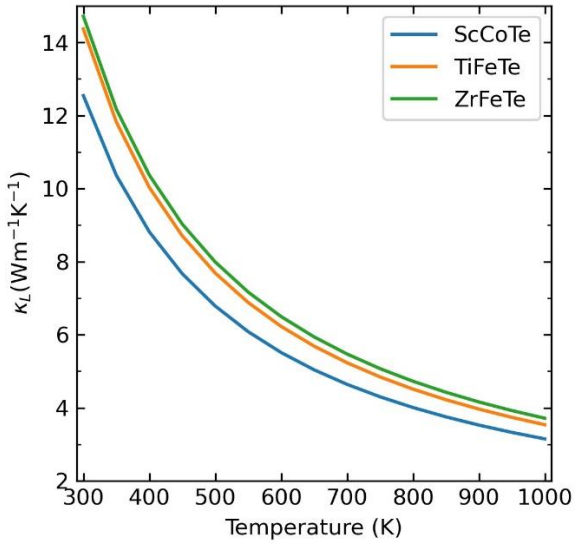

Figure S51: Lattice thermal conductivity of this group of compounds.

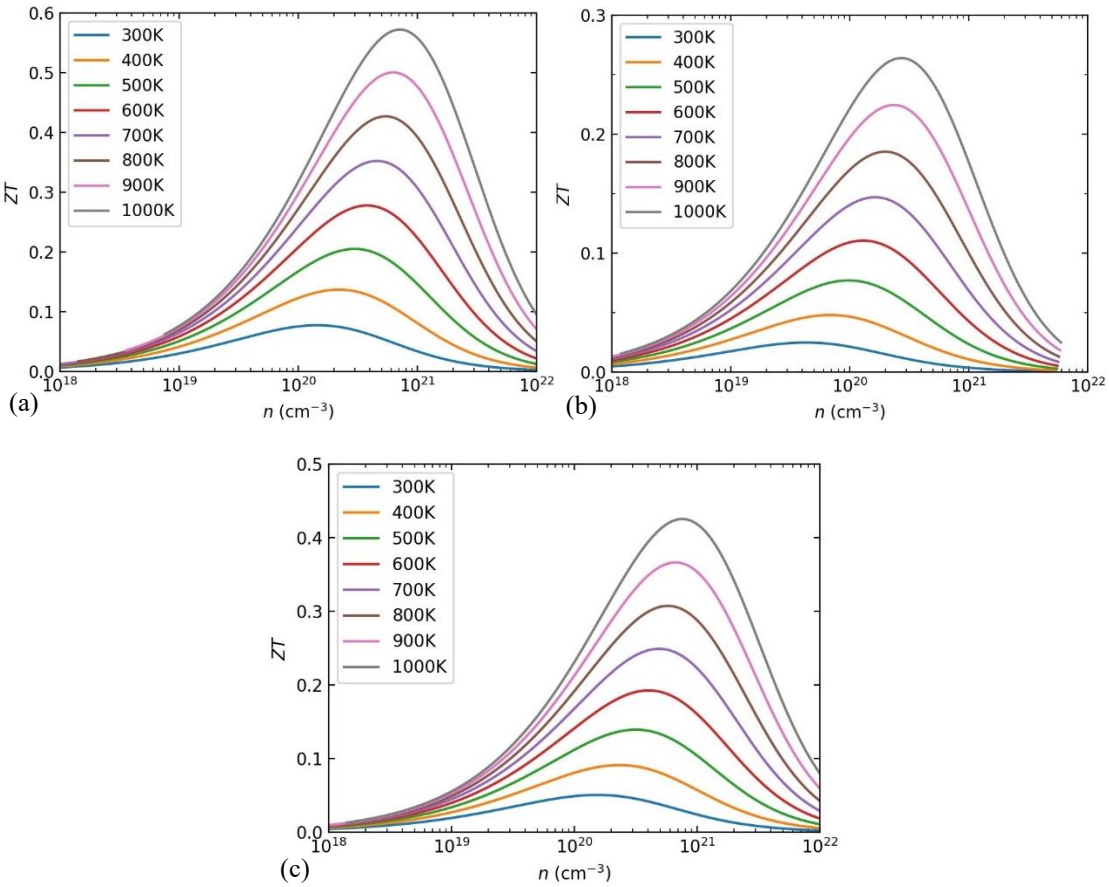

Figure S52: Figure of merit at varying temperatures and carrier concentrations for (a) ScCoTe, (b) TiFeTe, (c) ZrFeTe.

7. $Mg_2Co_4S_8$ and $Zn_2Co_4S_8$

These Two compounds have the same crystal structure (space group *F*d-3m), as shown in Fig. S53. According to our calculation, these two compounds have high power factor for both *n*- and *p*-type transport. The only problem is their lattice thermal conductivity are also high. Thus, the figure of merit of them are low.

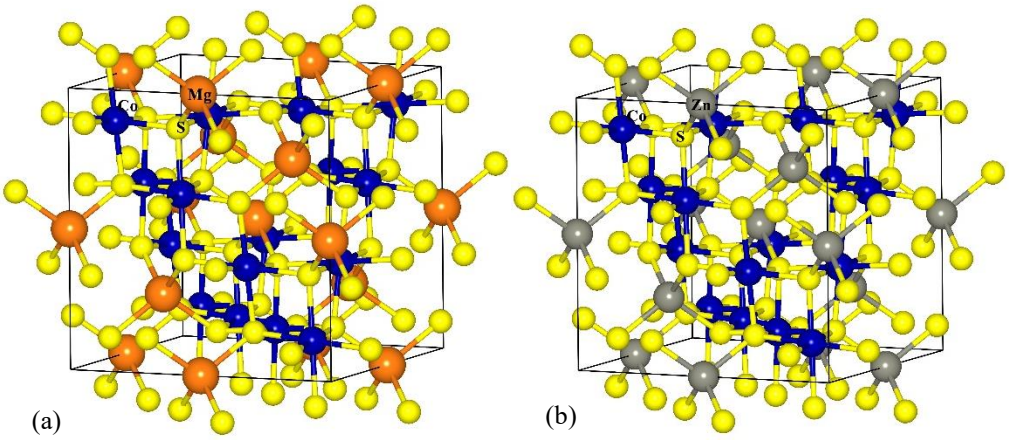

Figure S53: Crystal structures of (a) $Mg_2Co_4S_8$, (b) $Zn_2Co_4S_8$.

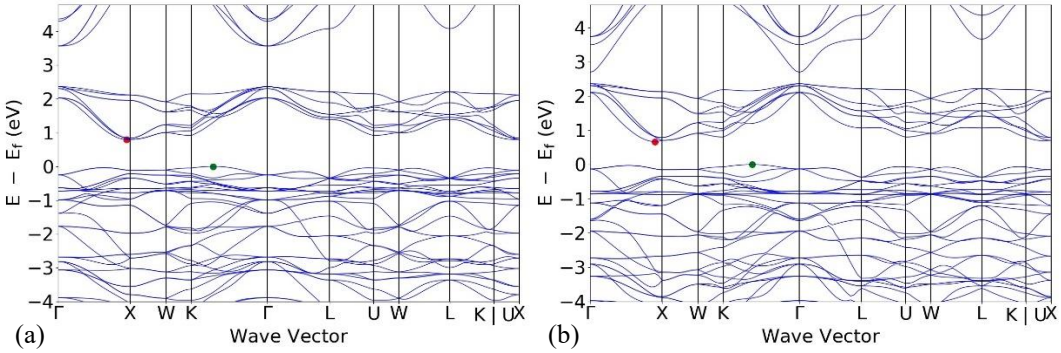

Figure S54: Band structures of (a) $Mg_2Co_4S_8$, (b) $Zn_2Co_4S_8$.

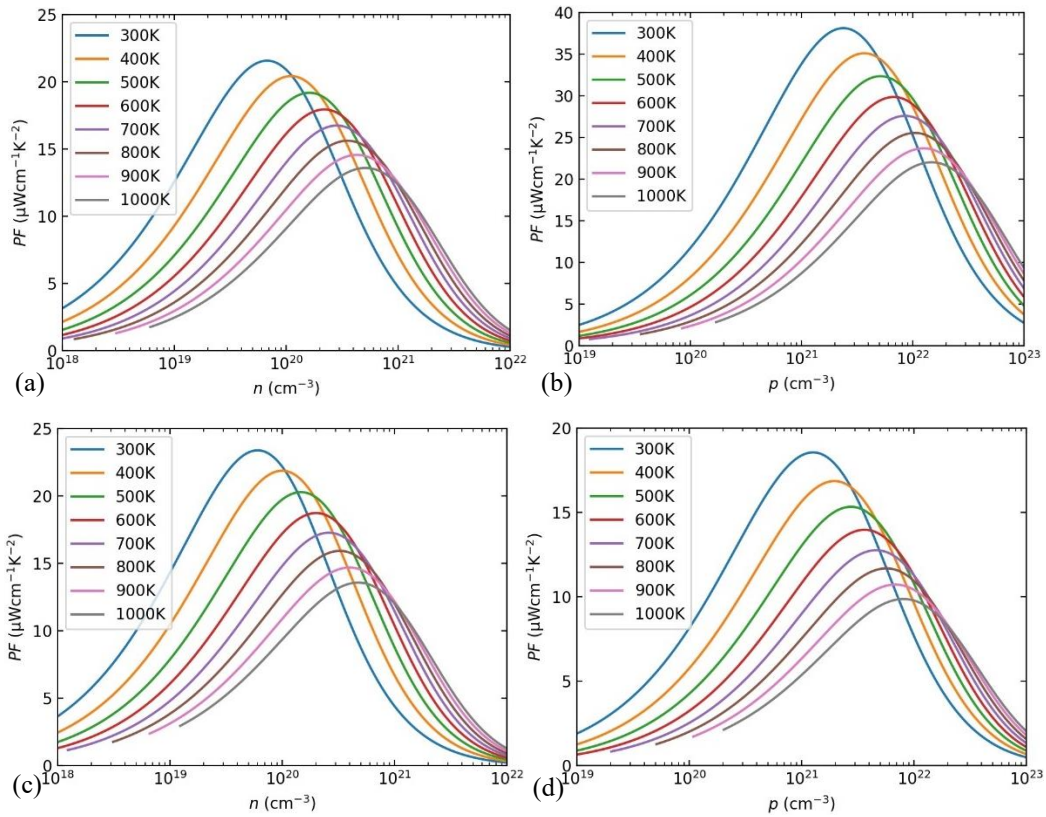

Figure S55: Power factor at varying temperatures and carrier concentrations for (a)(b) $Mg_2Co_4S_8$, (c)(d) $Zn_2Co_4S_8$.

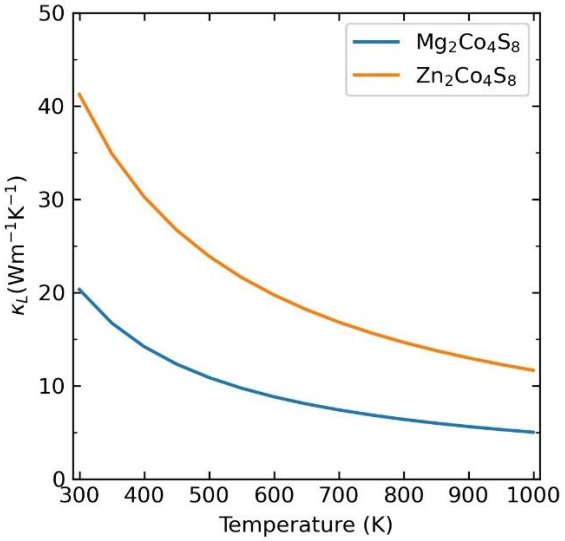

Figure S56: Lattice thermal conductivity of this group of compounds.

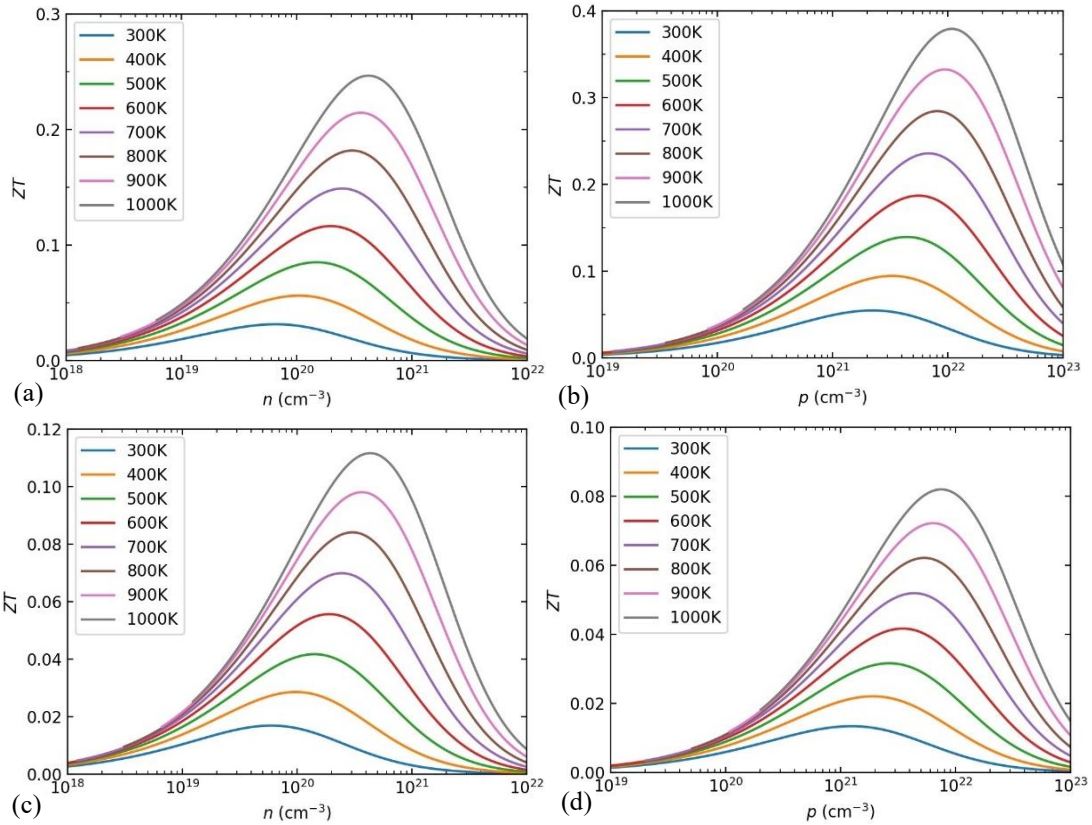

Figure S57: Figure of merit at varying temperatures and carrier concentrations for (a)(b) $Mg_2Co_4S_8$, (c)(d) $Zn_2Co_4S_8$.

8. Al_5CuSe_8

This compound has a structure with space group *F*-43m, as shown in Fig. S58. According to our calculation, it is promising for *p*-type thermoelectric materials.

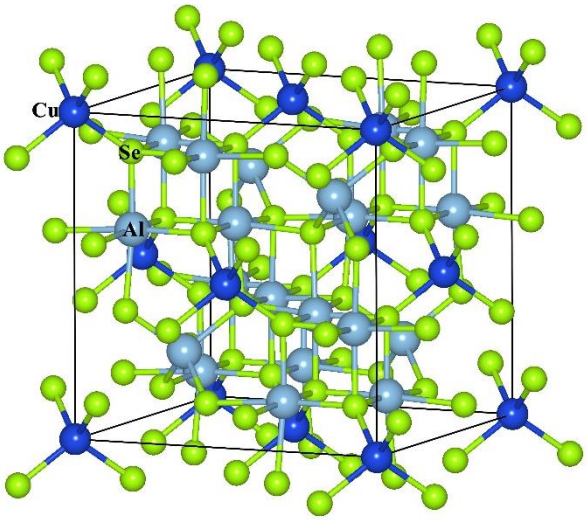

Figure S58: Crystal structure of Al_5CuSe_8.

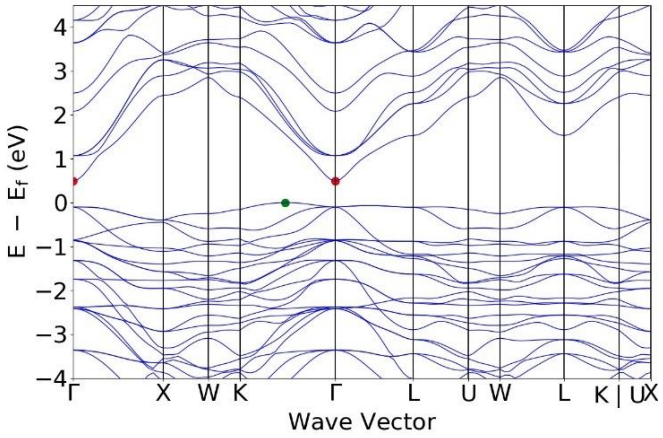

Figure S59: Band structure of Al_5CuSe_8.

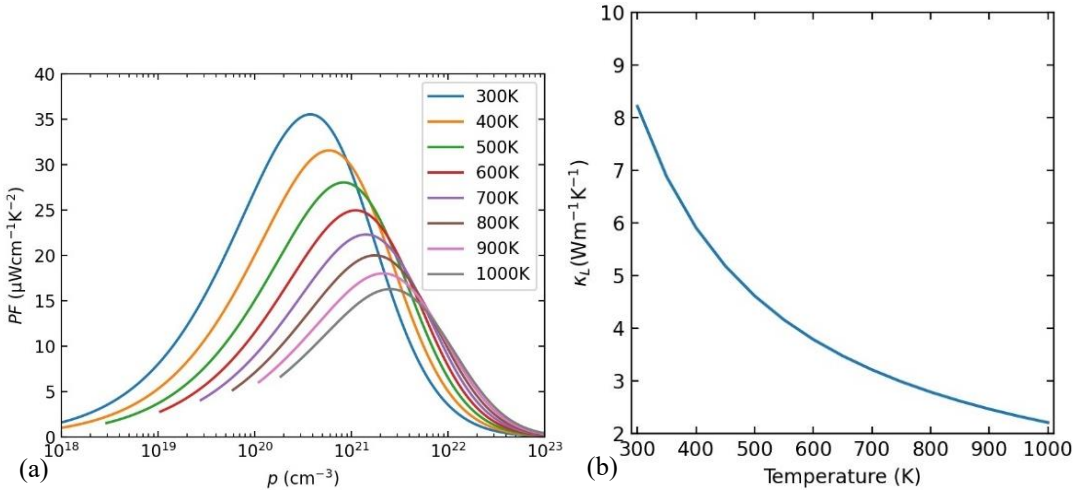

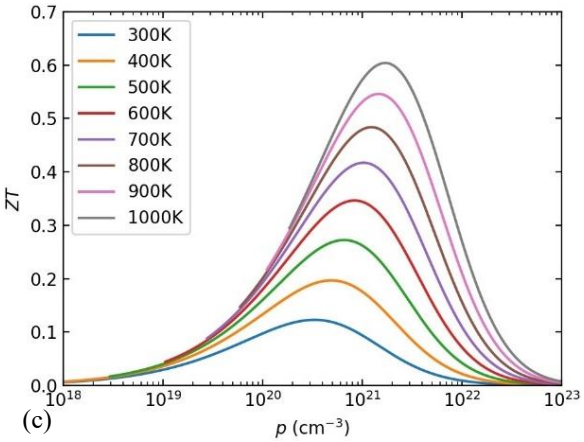

(c)

Figure S60: Thermoelectric properties of Al_5CuSe_8 for *p*-type transport. (a) power factor, (b) lattice thermal conductivity, (c) figure of merit.

9. Ce_4Se_8

This compound has a structure with space group *F*d-3m, as shown in Fig. S61. According to our calculation, it is promising for *p*-type thermoelectric materials.

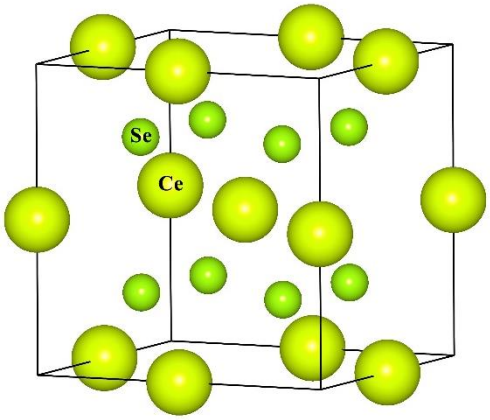

Figure S61: Crystal structure of Ce_4Se_8.

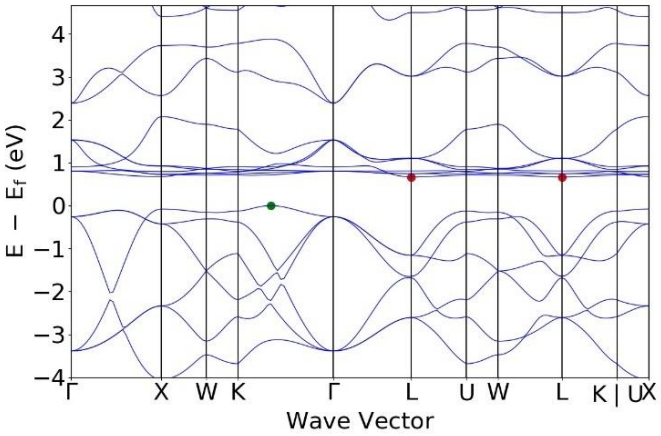

Figure S62: Band structure of Ce_4Se_8.

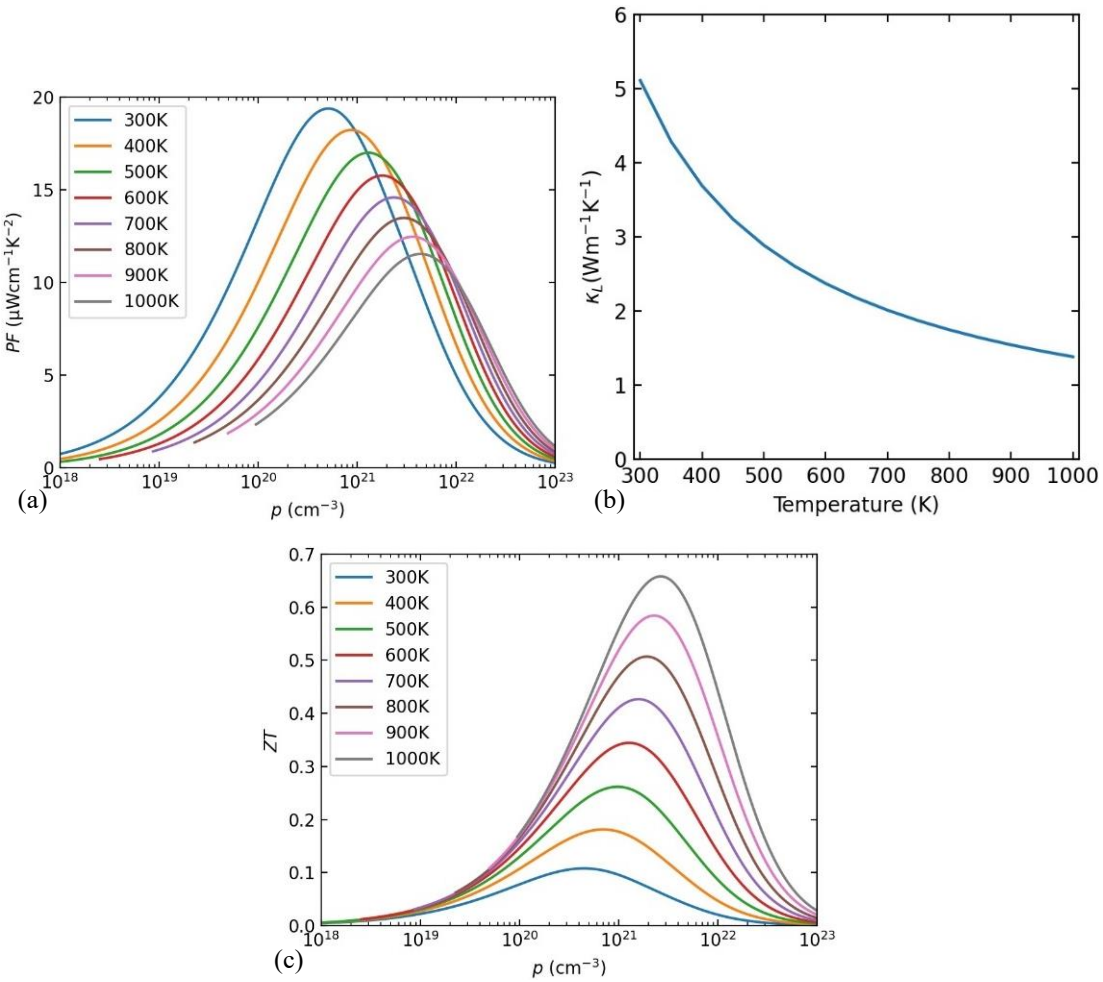

Figure S63: Thermoelectric properties of Ce_4Se_8 for *p*-type transport. (a) power factor, (b) lattice thermal conductivity, (c) figure of merit.

10. $Y_4Pt_4S_{14}$

This compound has a structure with space group *F*d-3m, as shown in Fig. S64. According to our calculation, it is promising for *p*-type thermoelectric materials.

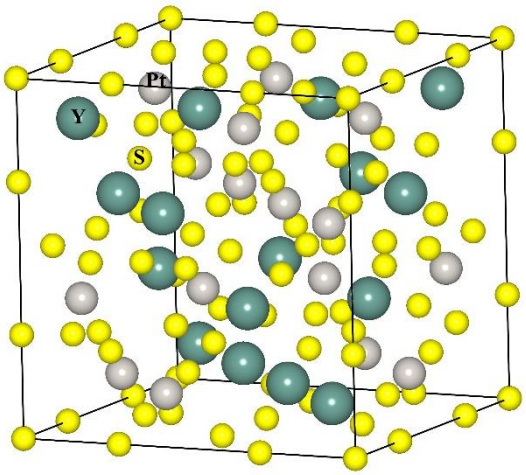

Figure S64: Crystal structure of $Y_4Pt_4S_{14}$.

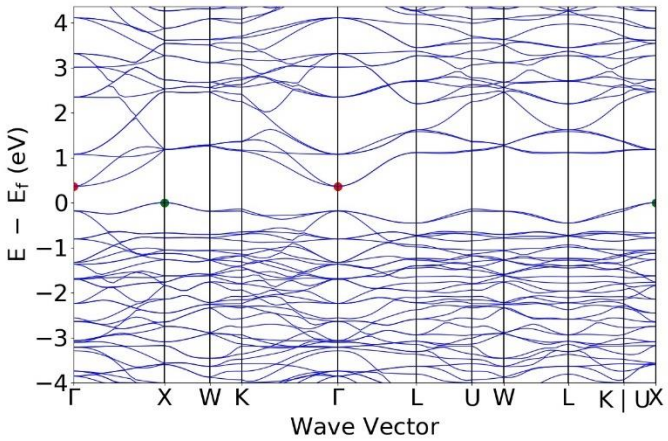

Figure S65: Band structure of $Y_4Pt_4S_{14}$.

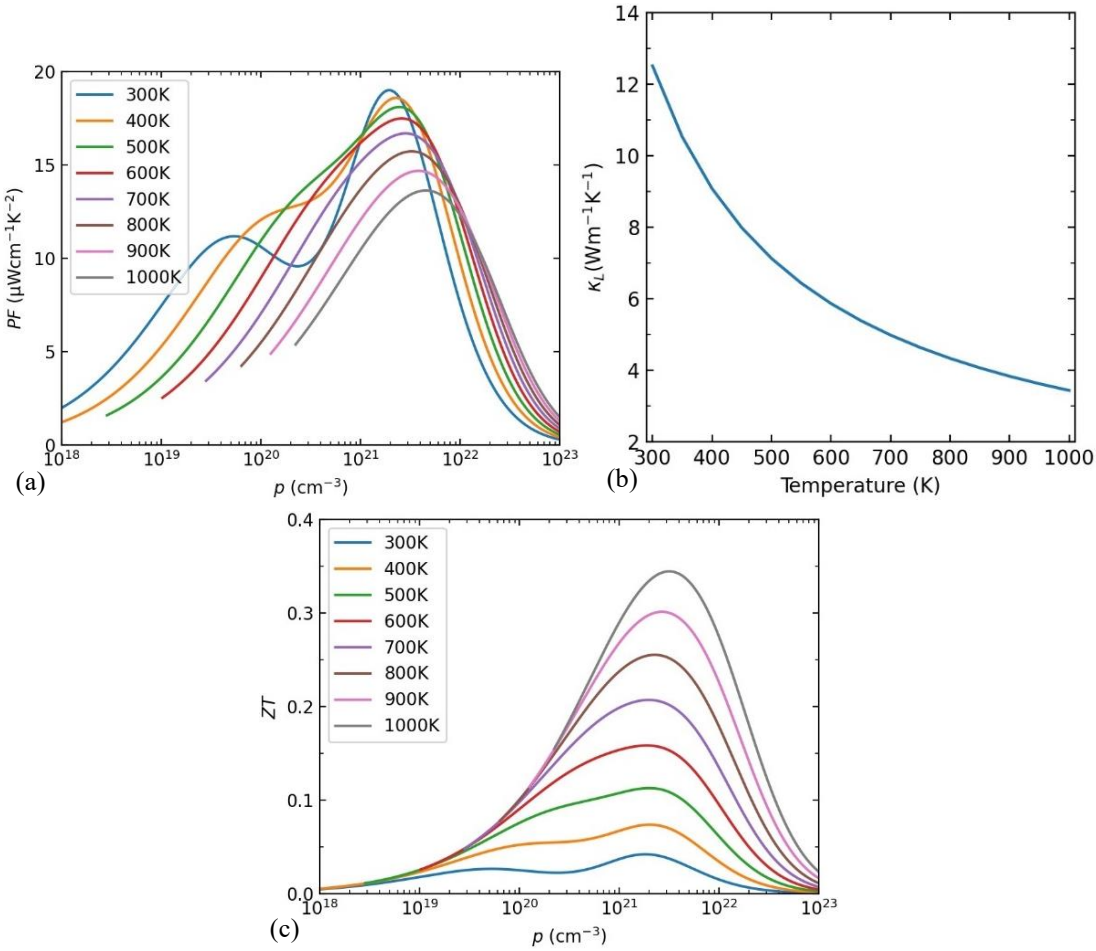

Figure S66: Thermoelectric properties of $Y_4Pt_4S_{14}$ for *p*-type transport. (a) power factor, (b) lattice thermal conductivity, (c) figure of merit.

11. $Li_4Co_4S_8$

This compound has a structure with space group *F*d-3m, as shown in Fig. S67. According to our calculation, it is promising for *p*-type thermoelectric materials.

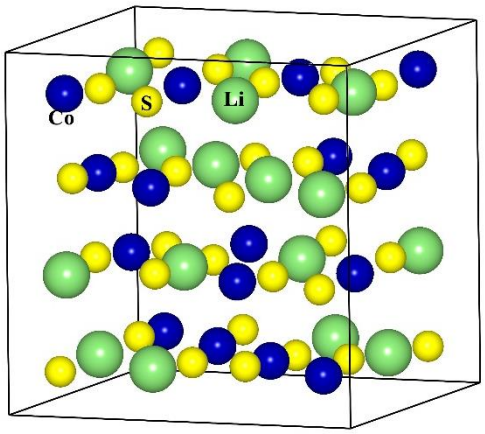

Figure S67: Crystal structure of $Li_4Co_4S_8$.

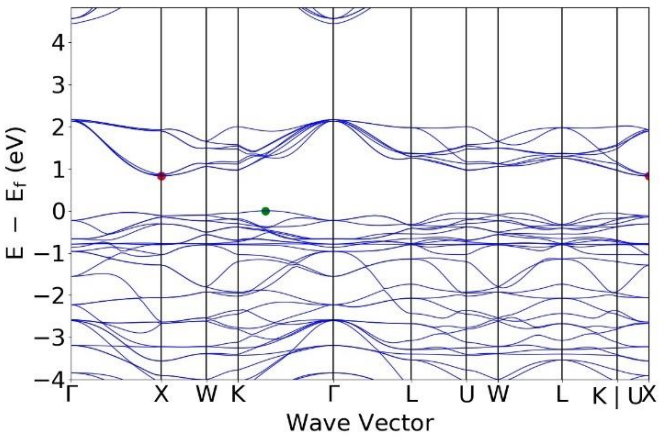

Figure S68: Band structure of $Li_4Co_4S_8$.

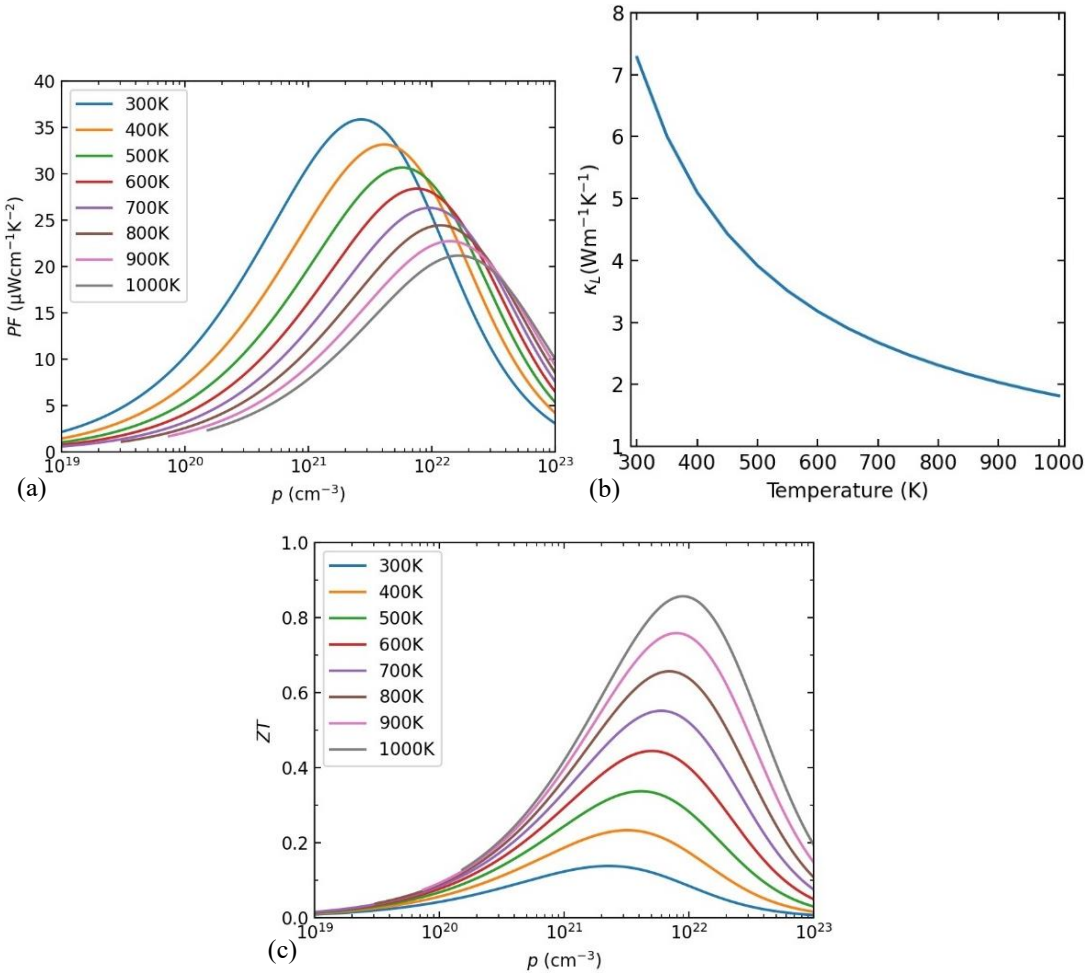

Figure S69: Thermoelectric properties of $Li_4Co_4S_8$ for *p*-type transport. (a) power factor, (b) lattice thermal conductivity, (c) figure of merit.

12. $Nb_6Sb_4Te_{10}$

This compound has a structure with space group *I*-43m, as shown in Fig. S670. According to our calculation, it is promising for *p*-type thermoelectric materials.

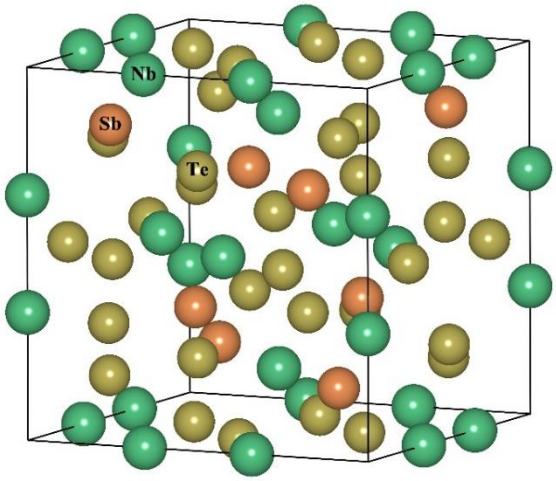

Figure S70: Crystal structure of $Nb_6Sb_4Te_{10}$.

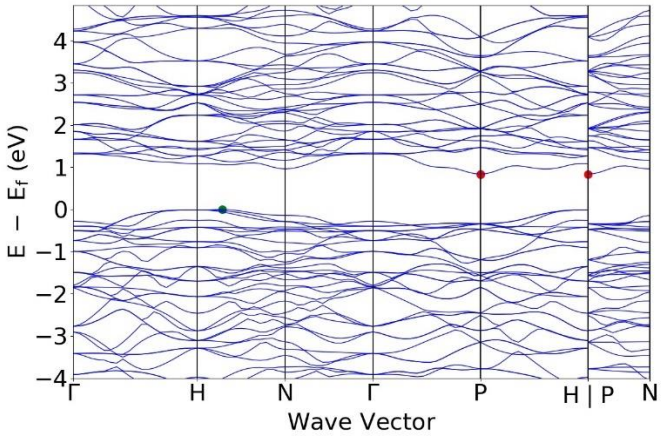

Figure S71: Band structure of $Nb_6Sb_4Te_{10}$.

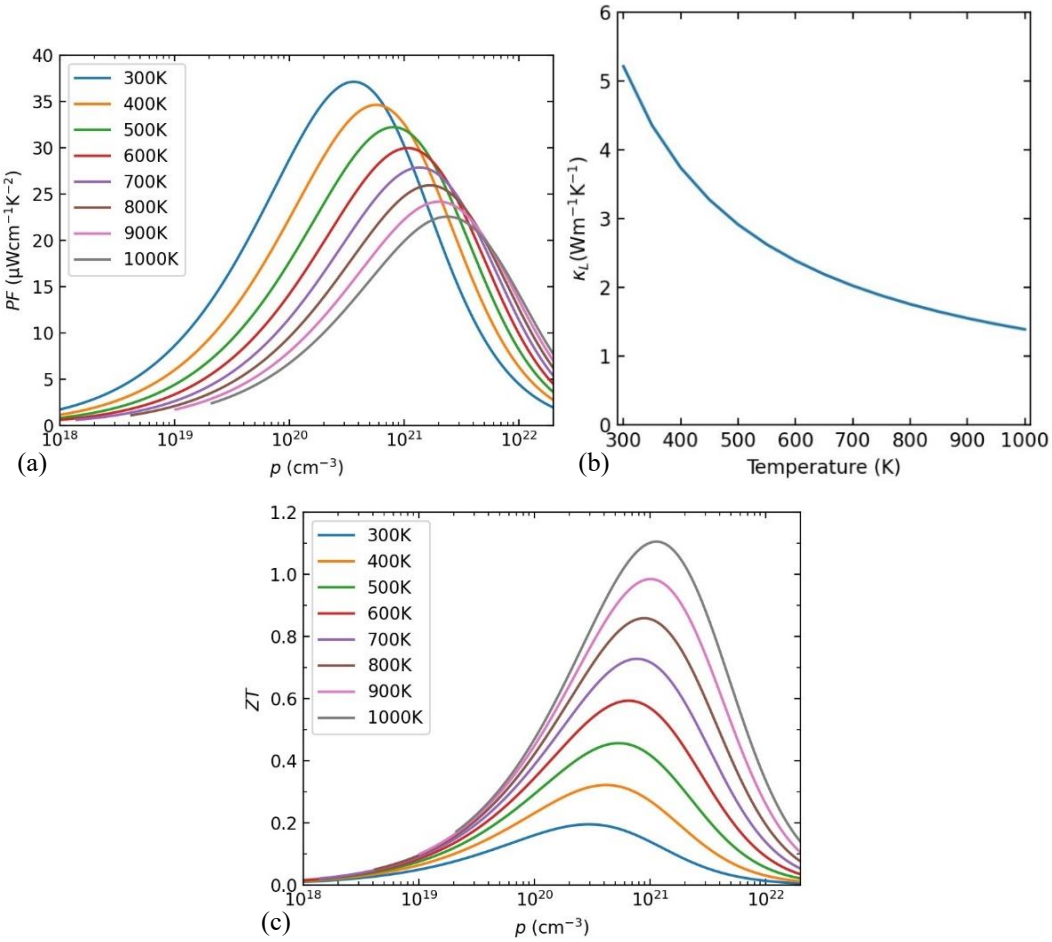

Figure S72: Thermoelectric properties of $Nb_6Sb_4Te_{10}$ for *p*-type transport. (a) power factor, (b) lattice thermal conductivity, (c) figure of merit.

13. MgTe

This compound has a structure with space group *F*m-3m, as shown in Fig. S73. According to our calculation, this compound has high power factor for both *n*- and *p*-type transport, especially for *p*-type. Figure of merit of *p*-type could be above 1 at high temperature.

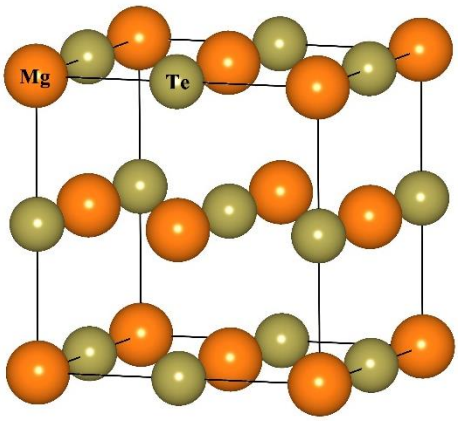

Figure S73: Crystal structure of MgTe.

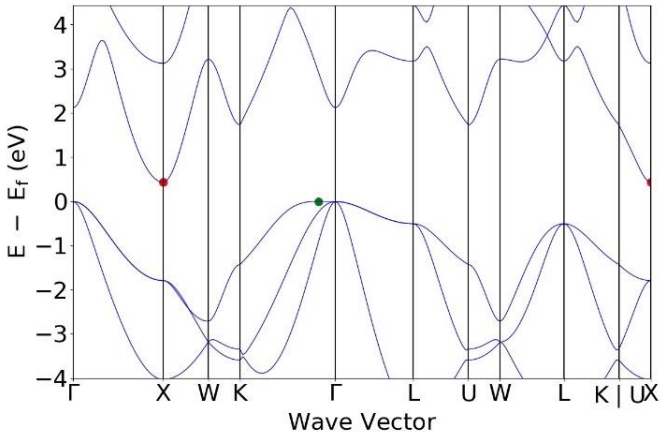

Figure S74: Band structure of MgTe.

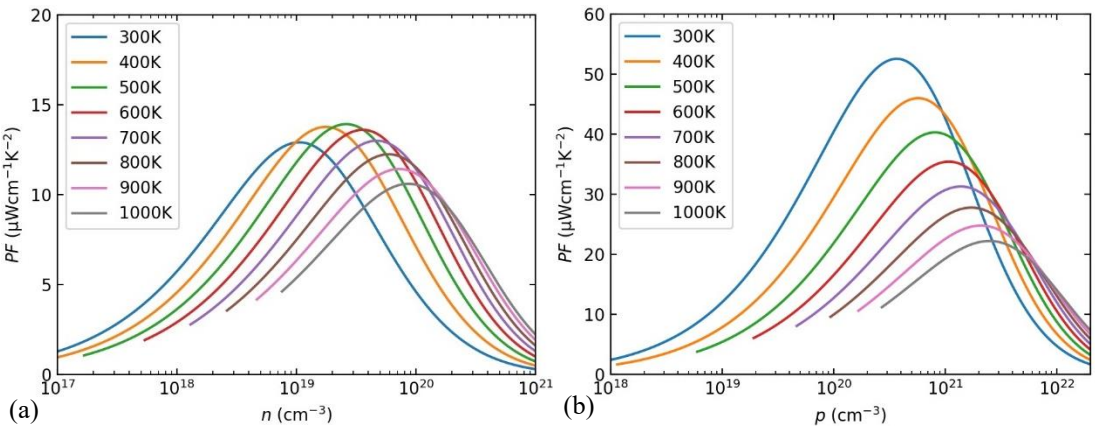

Figure S75: Power factor at varying temperatures and carrier concentrations for MgTe.

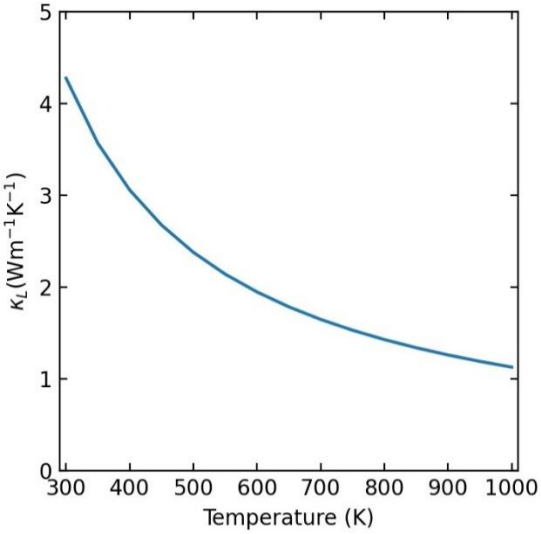

Figure S76: Lattice thermal conductivity of MgTe.

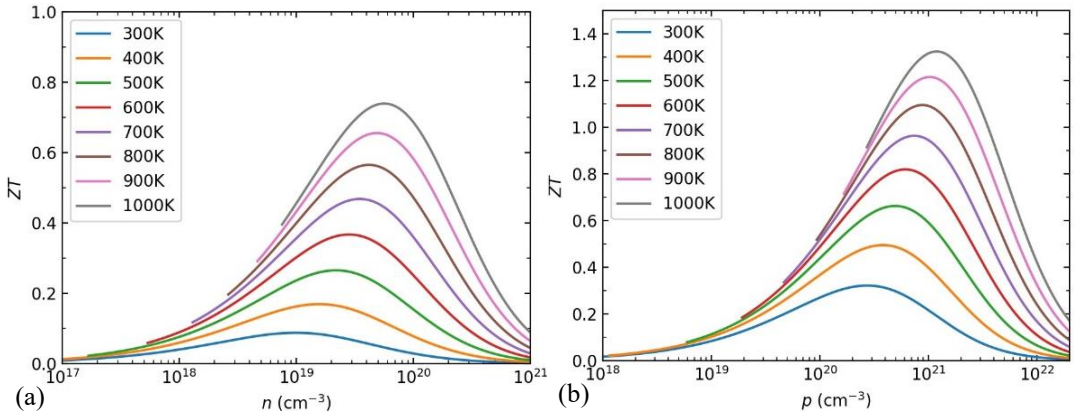

Figure S77: Figure of merit at varying temperatures and carrier concentrations for MgTe.